INVESTIGATION OF THE EFFECT OF V-SET TRANSMEMBRANE DOMAIN CONTAINING-5 (VSTM5) PROTEIN ON THE GROWTH RATE OF CONSENSUS MOLECULAR SUBTYPE -1 (CMS1) GROUP COLON ADENOCARCINOMA CELL LINE CELLS

ADILE BUSE ANDAC-AKTAS

Thesis for the Master's Program in Bioengineering

Graduate School
Izmir University of Economics
Izmir
2023

INVESTIGATION OF THE EFFECT OF V-SET TRANSMEMBRANE DOMAIN CONTAINING-5 (VSTM5) PROTEIN ON THE GROWTH RATE OF CONSENSUS MOLECULAR SUBTYPE -1 (CMS1) GROUP COLON ADENOCARCINOMA CELL LINE CELLS

ADILE BUSE ANDAC-AKTAS

THESIS ADVISOR: ASSOC. PROF. DR. B. EMRE DAYANÇ
CO-ADVISOR: ASSOC. PROF. DR. OSMAN DOLUCA

A Master's Thesis
Submitted to
the Graduate School of Izmir University of Economics
the Department of Bioengineering

Izmir
2023

ETHICAL DECLARATION

I hereby declare that I am the sole author of this thesis and that I have conducted my work in accordance with academic rules and ethical behavior at every stage from the planning of the thesis to its defense. I confirm that I have cited all ideas, information and findings that are not specific to my study, as required by the code of ethical behavior, and that all statements not cited are my own.

Name, Surname:
ADILE BUSE ANDAC-AKTAS
Date:
19.10.2023

Signature:

ABSTRACT

INVESTIGATION OF THE EFFECT OF V-SET TRANSMEMBRANE DOMAINS CONTAINING-5 (VSTM5) PROTEIN ON THE GROWTH RATE OF CONSENSUS MOLECULAR SUBTYPE -1 (CMS1) GROUP COLON ADENOCARCINOMA CELL LINE CELLS,

Andac-Aktas, Buse Adile

Master's Program in Bioengineering

Advisor: Assoc. Prof. Dr. B. Emre DAYANC
Co-Advisor: Assoc. Prof. Dr. Osman DOLUCA

October, 2023

The classification of colon cancer patients into consensus molecular subtypes (CMS) is a recent protocol that has yet to be integrated into clinical practice guidelines. The anticipation of this classification contributing to the determination of treatment approaches by aiding in the prediction of the disease's prognosis augments the interest in this subject for translational research. At present, prognosticating disease outcome is becoming increasingly significant in clinical decision-making systems, compelling the use of molecular markers. Our team's in-silico investigations have revealed that the VSTM5 gene, which is positively associated with survival in CMS1 group colon cancer patients, has an impact on neural development, immunosuppressive effects on cytotoxic T lymphocytes, and restrains T cell proliferation. This thesis explores the potential dual mechanisms underlying the influence of the VSTM5 gene on survival. Specifically, the investigation focuses on the impact of the VSTM5 gene on the growth

rate of colon cancer cells. For this purpose, we determined the basal expression levels of VSTM5 in CMS1 group of colon cancer cell lines and cloned the coding sequence of VSTM5 to the mammalian expression vector pcDNA3-EGFP. The results of this research endeavor are expected to make a valuable contribution to the existing literature on the limitedly studied effects of the VSTM5 gene on the growth of CMS1 group colon cancer cell lines and its consequent impact on survival.

Keywords: VSTM5, CMS1, Colon cancer, survival rate, cell growth rate.

ÖZET

V-SET TRANSMEMBRAN DOMAİN İÇEREN-5 (VSTM5) PROTEİNİNİN KONSENSÜS MOLEKÜLER ALT TIP-1 (CMS1) GRUBU KOLON ADENOKARSİNOMA HÜCRE HATTI HÜCRELERİNİN BÜYÜME HIZINA ETKİSİNİN İNCELENMESİ

Andac-Aktas, Buse Adile

Biyomühendislik Yüksek Lisans Programı

Tez Danışmanı: Doç. Dr. B. Emre Dayanc
Tez İkinci Danışmanı: Doç. Dr. Osman Doluca

Ekim, 2023

Kolon kanseri hastalarının konsensüs moleküler alt tiplere (CMS) sınıflandırılması yeni bir yaklaşım olup, henüz bu hastalığın klinik pratik rehberlerine girmemiştir. Bu sınıflandırmanın, hastalığın prognozunun öngörülmesine yardımcı olarak tedavi yaklaşımlarının belirlenmesine katkı vermesi beklentisi, translasyonel araştırmalar için konuya ilgiyi arttırmaktadır. Günümüzde kullanılan klinik karar destek sistemlerinde hastalık prognozunu öngörmek önem kazanmakta ve bu amaçla moleküler belirteçlere ihtiyaç duyulmaktadır. Çalışma ekibimizin yaptığı *in silico* çalışmalarda, CMS1 grubu kolon kanseri hastalarında sağkalım süresi ile pozitif korelasyon gösteren VSTM5 geninin, nöral gelişim üzerinde etkisi olduğu, sitotoksik T lenfositleri üzerinde immünosupresif etkisi olduğu ve T hücre proliferasyonunu inhibe ettiği bildirilmiştir. VSTM5 geninin sağkalıma etkisinin farklı mekanizmalar

ile olabileceği değerlendirip, bunlardan en temeli olan kolon kanseri hücrelerinin bölünme hızına etkisinin bu tez kapsamında incelenmesi amaçlanmıştır. Bu amaçla, kolon kanseri hücre hatlarının CMS1 grubundaki VSTM5'in bazal ekspresyon düzeylerini belirledik ve VSTM5'in kodlayıcı dizisini memeli ifade vektörü pcDNA3-EGFP'ye klonladık. Elde edilen sonuçların, literatürde kısıtlı çalışmaya sahip olan VSTM5 geninin, CMS1 grubu kolon kanseri hücre hatlarının büyümesine etkisi hakkında literatüre katkı sağlaması ve sağkalıma etkisini açıklayabilecek diğer çalışmalara öncü olması beklenmektedir.

Anahtar Kelimeler: VSTM5, CMS1, Kolon kanseri, sağkalım, hücre büyümesi.

Dedicated to my beloved family, and with boundless gratitude and love, to my dear mother who holds a special place in my heart.

ACKNOWLEDGEMENTS

I am immensely grateful to my advisor, Assoc. Prof. Dr B. Emre Dayanç, for his invaluable expertise, mentorship, and unwavering support throughout my research endeavor. I am sincerely grateful for his relentless commitment to both my personal and academic development. I extend my sincerest thanks to my co-advisor, Associate Professor Osman Doluca, for his valuable contributions and constructive feedback.

I express my gratitude to H. Saygın Portakal and Sıla Naz Köse for their cooperation, assistance, unwavering backing, and skillful troubleshooting during my thesis experiments. Their support and willingness to lend a helping hand were truly priceless. I am appreciative of the countless hours we spent in the laboratory, brainstorming, resolving experimental challenges, providing encouragement, and celebrating our collective achievements.

I am immensely grateful to my father, Yüksel Andaç, and brother, Ege Kaan Andaç, for their boundless affection, unwavering valor, and steadfast confidence in my capabilities. Their consistent backing, comprehension, and fortitude have been a source of vigor and incentive. I wholeheartedly value their selflessness which facilitated me to pursue my academic objectives and continue this research odyssey. Their relentless support has established the foundation for my triumph, and I am truly fortunate to have them by my side.

I wish to express my sincere gratitude to my spouse, Okan Aktaş, for his valiant devotion, unconditional endorsement, and profound perception throughout this expedition. Even during moments of self-doubt, his perseverance and unwavering belief in my potential have been my source of vigor. I am truly privileged to have him as my life partner.

Finally, I would like to honor the memory of my beloved mother, Ayşe Andaç, who passed away. Her unwavering backing and the principles she ingrained in me shall forever be appreciated. Her legacy shall serve as a guiding force as I aspire to effectuate a significant contribution in the battle against cancer.

TABLE OF CONTENTS

LIST OF TABLES

LIST OF FIGURES

ABBREVIATIONS

18S rRNA: 18S Ribosomal RNA

A549: Lung cancer cell line

aa: Amino acids

ABM: Applied Biological Materials Inc.

Amp: Ampicillin (antibiotic)

B cells: B lymphocytes

BRAF: B-Raf proto-oncogene, serine/threonine kinase

Buffer RA3: Elution buffer

Buffer RAW2: Wash buffer

CCD18-Co: Colon epithelial cell line

CD112: Cluster of Differentiation 112 (also known as PVRL2 or nectin-2)

CD150: Cluster of Differentiation 150

CD155: Cluster of Differentiation 155 (also known as PVR, poliovirus receptor)

CD244: Cluster of Differentiation 244

CD48: Cluster of Differentiation 48

CD8A: Cluster of Differentiation 8A

Cdc42: Cell division control protein 42

cDNA: Complementary DNA

CECAM21: Carcinoembryonic Antigen-related Cell Adhesion Molecule 21

CIMP: CpG island methylator phenotype

CIN: Chromosomal instability

CK2: Casein Kinase-2

CMS: Consensus molecular subtypes

CMS1: Consensus Molecular Subtype 1

CMS2: Consensus Molecular Subtype 2

CMS3: Consensus Molecular Subtype 3

CMS4: Consensus Molecular Subtype 4

CO2: Carbon dioxide

CRC: Colorectal cancer

CRP: C-reactive protein

CRT: Chemoradiotherapy

Ct: Cycle Threshold

DH5α: Escherichia coli DH5α

DMEM: Dulbecco's Modified Eagle Medium

DMR: Differentially methylated regions

DMSO: Dimethyl sulfoxide

DNAM-1: DNAX accessory molecule 1

DNase: Deoxyribonuclease

dNTP: Deoxynucleotide triphosphate

ECD: Extracellular domain

EDTA: Ethylenediaminetetraacetic acid

ELM: Eukaryotic Linear Motif

EMT: Epithelial-to-mesenchymal transition

Eppendorf: A type of laboratory tube

EtBr: Ethidium Bromide

ExPASY: Expert Protein Analysis System

F-actin: Filamentous actin

FBS: Fetal Bovine Serum

GEO: Gene Expression Omnibus

GZMA: Granzyme A

H2O: Water

HADDOCK: High Ambiguity Driven protein-protein DOCKing

HCT116: Colorectal cancer cell line

HIV: Human immunodeficiency virus

HPV: Human papillomavirus

HT29: A colon cancer cell line derived from human colorectal adenocarcinoma

IBD: Inflammatory bowel disease

IFN-y: Interferon-gamma

Ig: Immunoglobulin

IgSF: Immunoglobulin superfamily

IL-17: Interleukin-17

IL-17A: Interleukin 17A

IL-2: Interleukin-2

IL-4: Interleukin-4

ITIM: Immunoreceptor tyrosine-based inhibitory motif

ITSM: Immunoreceptor tyrosine-based switch motif

ITT: Ig tail-tyrosine

KRAS: Kirsten rat sarcoma viral oncogene homolog

LARC: Locally Advanced Rectal Cancer

LB Agar-Amp: Luria-Bertani Agar with Ampicillin

LB: Luria-Bertani (culture medium)

LoVo: Colorectal cancer cell line

MDB: Membrane Desalting Buffer

MHC: Major Histocompatibility Complex

MII5: Meiotic Spindle Checkpoint Protein

mRNA: Messenger RNA

MSI: Microsatellite instability

MYC: Myelocytomatosis oncogene

NF-κB: nuclear factor kappa B

NK: Natural killer

OPSCC: Oropharyngeal squamous cell carcinoma

PBLs: peripheral blood lymphocytes

PBMC: peripheral blood mononuclear cells

PBS: Phosphate-buffered saline

pcDNA3-EGFP: Plasmid vector with EGFP (Enhanced Green Fluorescent Protein) gene

PCR: Polymerase Chain Reaction

pCRT: Preoperative Chemoradiotherapy

PDB: Protein Data Bank

Penicillin-Streptomycin: A combination of the antibiotics penicillin and streptomycin

POD: Post-operative delirium

PRF1: Perforin-1

qPCR: Quantitative Polymerase Chain Reaction

RA: Rheumatoid arthritis

RA1: Lysis buffer

RNA: Ribonucleic acid

RNase-free H2O: Ribonuclease-free water

RPM: Revolutions per minute

RT-qPCR: Reverse Transcription Quantitative Polymerase Chain Reaction

RT: Reverse transcription

RTase: Reverse transcriptase

SLAM: Signaling lymphocytic activation molecule

SOC medium: Super Optimal Broth with Catabolite Repression medium

SPPIDER II: Sequence-based Protein-Protein Interaction Database for Docking, Energetics, and Regulation

ß-ME: Beta-mercaptoethanol

STAT3: Signal Transducer and Activator of Transcription 3

T cell: T lymphocyte

TAE buffer: Tris-Acetate-EDTA buffer

TE buffer: Tris-EDTA buffer

TGF-β: Transforming growth factor-beta

TIGIT: T-cell immunoreceptor with Ig and ITIM domain

TMB: Tumor Mutation Burden

TNF-α: Tumor necrosis factor-alpha

VEGF: Vascular endothelial growth factor

VSTM: V-set and transmembrane domain-containing

VSTM1: V-set and transmembrane domain-containing 1

VSTM1-v2: V-set and transmembrane domain-containing 1 variant 2

VSTM2: V-set and transmembrane domain-containing 2

VSTM2B: V-set and transmembrane domain-containing protein 2B

VSTM2L: V-set and transmembrane domain-containing 2-like

VSTM4: V-set and transmembrane domain-containing protein 4

VSTM5: V-Set and Transmembrane Domain Containing 5

γ-H2AX: Gamma-H2A.X (a marker for DNA double-strand breaks)

CHAPTER 1: INTRODUCTION

1.1. Colon Cancer Epidemiology and Carcinogenesis

Colorectal cancer is an important public health issue worldwide, being the second most common cancer in women and the third most common cancer in men. The disease causes an average of 600,000 deaths per year (Kuipers et al., 2015). In 2020, 1,148,515 new cases of colorectal cancer were reported, resulting in 576,858 deaths (Sung et al., 2021). Colorectal cancer incidence and mortality vary geographically, with the highest incidence rates found in Australia and New Zealand, and the lowest distribution in West Africa. Colon cancer ortality is influenced by the availability and level of care provided in each country (Kuipers et al., 2015).

Colon cancer epidemiological studies point out that developed regions demonstrate greater mortality rates when compared to less developed regions. Additionally, it has been noted that nations with greater survival rates commonly exhibit a high occurrence of colon cancer. This phenomenon can be attributed to the early detection facilitated by population screening programs. Several countries have implemented screening programs, which include a "fecal occult blood test" that is recommended for individuals aged 50 to 70 every two years. In addition, colonoscopies are recommended every ten years as a follow-up screening after age 50.

In Turkey, the fecal occult blood test is available for colon cancer screening at public health centers. It is highly advisable that persons between the ages of 50 and 70 undergo this test biennially. Colonoscopy is suggested to be conducted every ten years after attaining the age of 50. These screening measures play a crucial role in the early identification and management of colon cancer (Hacıkamiloğlu et al., 2017).

Colon cancer’s incidence and mortality rates are impacted by diverse factors, encompassing lifestyle and environmental influences. According to research, certain choices in lifestyle have been demonstrated to increase the possibility of colon cancer. The consumption of processed red meat, tobacco use, alcohol consumption, and a sedentary lifestyle are all factors that have been found to have a strong association with an increased risk of colon cancer. Furthermore, environmental factors, such as air and water pollution, could contribute to colon cancer's development. (Rawla et al., 2019).

Raising public consciousness, advocating for healthy lifestyle options, and executing efficacious screening protocols are among the methodologies that can be

utilized to curtail the prevalence and fatality of colon cancer. Additionally, patients afflicted with colon cancer have benefited from innovative medical technology and treatment alternatives.

In summary, colon cancer is a worldwide health issue, with dissimilar occurrence and mortality ratios across divergent regions. The importance of screening programs, like fecal occult blood tests and colonoscopies, in detecting and treating colon cancer at an early stage cannot be overstated. Lifestyle preferences and contribute to its onset. Augmenting public awareness, adopting wholesome lifestyles, and executing effective screening protocols are indispensable in diminishing the incidence and mortality rates of colon cancer. Therefore, it is crucial to enlighten the public about the significance of preventive healthcare and regular colon cancer screenings.

Colon cancer is the result of genetic or epigenetic alterations in epithelial cells that stimulate their proliferation (Testa et al., 2018). The development of polyps arises from the rapid proliferation of colon epithelial cells and can progress to cancer and metastasis through various mechanisms such as microsatellite instability (MSI), chromosomal instability (CIN), and serrated neoplasia (Figure 1). (Knudson, 1985; Kuipers et al., 2015; Testa et al., 2018)

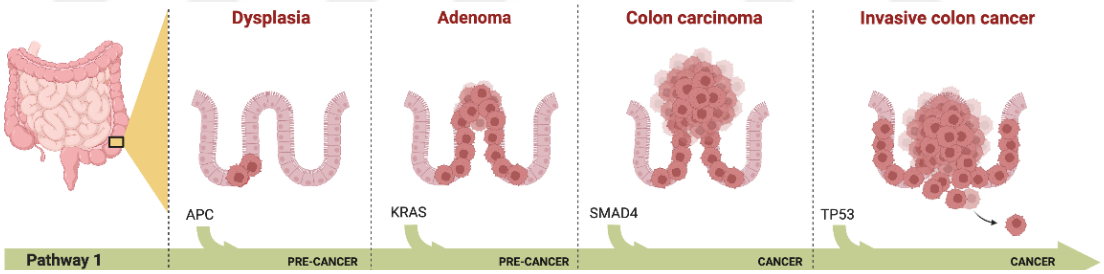

Figure 1. Colorectal cancer (CRC) stages and development. There are four stages in the development of CRC carcinogenesis: dysplasia, adenoma, colon carcinoma, and invasive colon cancer.

Extended inflammation is a major contributor to the formation of indeterminate dysplasia in normal cells, which advances from low-grade dysplasia to high-grade dysplasia and eventually to cancer (Keum and Giovannucci, 2019). Inadequate p53 signaling has been identified as an early event in the dysplasia-to-cancer transition. Colon cancer is associated with inflammatory bowel disease (IBD), with individuals affected by IBD being 2-6 times more susceptible to colon cancer than healthy individuals (Keller et al., 2019).

Chronic inflammation in IBD promotes colonic mucosa cell re-epithelialization, cell turnover, and potential errors in cell cycle repair. Once an adenocarcinoma has metastasized to other body parts, it can disseminate through the blood and lymphatic system. According to Pickhardt et al. (2013), adenocarcinomas account for approximately 96% of all colorectal cancers (CRCs) (Pickhardt et al., 2013). Like other types of tumors or cancers, CRC is staged from 0 (CIS- carcinoma in situ) to IV.

1.2. Classification of Colon Cancer

The global genomic status, including microsatellite instability (MSI) status and chromosomal instability (CIN) , as well as the epigenomic status, characterized by CpG island methylator phenotype (CIMP) , play a crucial role in determining the clinical, pathological, and biological features of colon cancer (Ogino and Goel, 2008). Traditionally, approximately 17% of colon cancers have been categorized as microsatellite instable (MSI), around 60% as chromosomal instable (CIN), and roughly 20% as CpG island methylation phenotype (CIMP) positive and with a fourth group that does not fit into these classifications (Walther et al., 2009). In recent years, colon cancer has been categorized into four consensus molecular subgroups (CMS). However, not all tumors still can be definitively assigned to all of these groups (Figure 2). The creation of CMS aimed to group colon cancer patient tumors based on independent assessments conducted by different research groups, utilizing various gene expression datasets and analytical methods. The diverse subgroups of CMS demonstrate unique features, such as a formidable immune response in CMS1, considerable chromosomal instability (CIN) in CMS2 and CMS4, various metabolic modifications in CMS3, and the presence of genes linked to the epithelial-to-mesenchymal transition (EMT) in CMS4.

CMS1 tumors are distinguished by a distinctive immune response, wherein lymphocytic reaction serves as a defining characteristic of this group. These tumors manifest elevated expression of genes linked to cytotoxic lymphocytes, such as CD8a, PRF1, and GZMA. Notably, CMS1 tumors display a heightened mutation burden, particularly in genes pertaining to the antigen presentation pathway. The observed augmented methylation in CMS1 tumors can be attributed to the high CpG island

methylator phenotype (CIMP), frequently associated with the BRAF mutation.

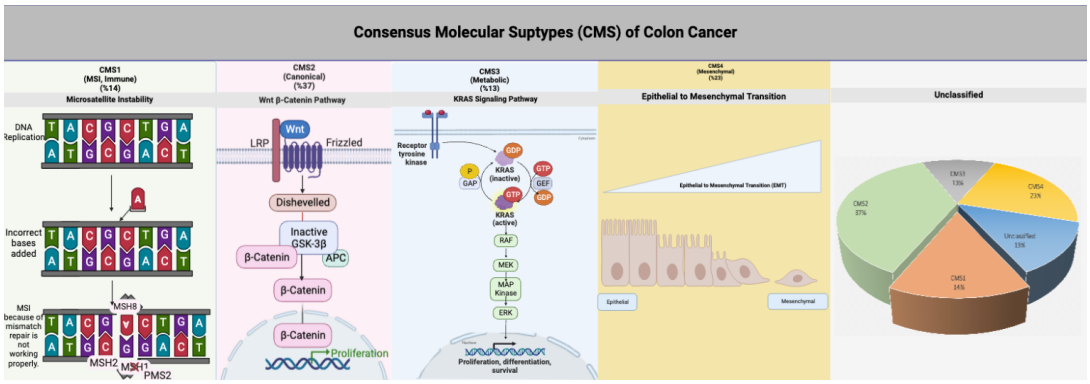

Figure 2. Consensus Molecular Subtypes. The creation of CMS aimed to group colon cancer patient tumors based on independent assessments conducted by different research groups, utilizing various gene expression datasets and analytical methods. Each CMS subgroup exhibits distinct characteristics, including a strong immune response in CMS1, high chromosomal instability (CIN) in both CMS2 and CMS4, multiple metabolic alterations in CMS3, and genes associated with the epithelial-to-mesenchyme transition (EMT) in CMS4.

Both CMS2 and CMS4 subgroups share high chromosomal instability (CIN), characterized by frequent chromosomal gains and losses. CMS2 tumors exhibit more frequent copy number gains in oncogenes and copy number losses in tumor suppressor genes than other subtypes. Moreover, CMS2 tumors display epithelial differentiation and excessive WNT and MYC signaling pathways activation. CMS4 tumors demonstrate alterations associated with the activation of the complement-mediated inflammatory system and increased signaling of TGF-β, which are involved in EMT.

CMS3 tumors are distinguished by multiple metabolic alterations, with KRAS-activating mutations known to induce significant metabolic adaptation. These tumors display a notable increase in fatty acid metabolism and a decrease in oxidative phosphorylation. The metabolic adaptation observed in CMS3 tumors is believed to be driven by the activation of oncogenic KRAS and the dysregulation of multiple signaling pathways.

Although the CMS classification has gained acceptance and has been incorporated into medical oncology textbooks (Dasari et al., 2022), its implementation in clinical practice is still pending. However, researchers have readily embraced this classification, leading to further investigations to clarify its clinical significance. In-silico investigations have played a pivotal role in grouping frequently utilized cell lines

into CMS categories. For example, the HCT116, HT29, and LoVo cell lines have been assigned to diverse CMS1 clusters in various studies (Fichtner et al., 2020). However, certain scholarly inquiries propose that the HCT116 cellular classifications categorized as CMS4 and HT29 have the potential to be classified as CMS3 (Berg et al., 2017). The ongoing research aims to establish a correlation between molecular subcategorization and its clinical applications.

In summary, the classification of colon cancer into consensus molecular subtypes (CMS) has provided valuable insights into the distinctive characteristics of these subtypes, offering a potential framework for tailored therapeutic approaches. CMS1 tumors exhibit a strong immune response, CMS2 and CMS4 tumors display high chromosomal instability (CIN), CMS3 tumors demonstrate multiple metabolic alterations, and CMS4 tumors exhibit alterations associated with complement-mediated inflammatory system activation and increased TGF-β signaling. This classification provides valuable insights into the molecular mechanisms underlying colon cancer and may pave the way for personalized treatment strategies tailored to specific subgroups of patients (Guinney et al., 2015).

1.3. VSTM Gene Family

The V-set and transmembrane domain-containing (VSTM) gene family, a ubiquitous group of genes, is recognized for its fundamental role in immune system regulation, thereby ensuring optimal health and immune protection. This suggests that these genes are important for keeping our immune system working effectively. Their critical functions range from pathogen recognition to immune response activation and immune memory maintenance. Additionally, some VSTM genes are responsible for cytokine production, which serves as a crucial aspect of immune system regulation. Furthermore, certain VSTM genes play an active role in the development of our immune system, specifically in the maturation of B and T cells. Therefore, it is clear why the VSTM gene family is so essential for the proper functioning of the immune system.

1.3.1. VSTM1:

V-set and transmembrane domain-containing 1 (VSTM1) functions significantly in the detection and signaling of antigens, along with the control of cytokine production and T-cell activation.

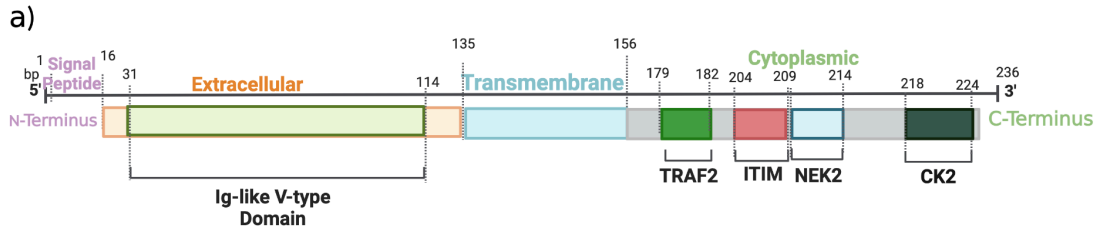

Figure 3. Structure of VSTM1. The extracellular region of VSTM1 contains an Ig-like V-type domain. In the cytoplasmic region, several motifs have been identified, including TRAF2, ITIM, NEK2, and CK2.

VSTM1 contains two primary isoforms, VSTM1-v1 and VSTM1-v2, as a soluble isoform. The former is predominantly expressed in human peripheral blood granulocytes and monocytes and has been identified as a neutrophil and monocyte inhibitor of IgSF (immunoglobulin superfamily) (Li et al., 2013; Steevels et al., 2010). The protein of type-1 membrane possesses an Ig-V domain and a pair of immunoreceptor tyrosine-based inhibitory motif (ITIM) (Figure 3). Conversely, VSTM1-v2 is a conventional secretory protein without the presence of a transmembrane domain. Its expression is primarily observed in immune cells and has been recognized as a cytokine. (Guo et al., 2012; Wang et al., 2016).

Although VSTM1 is widely expressed in normal human peripheral blood lymphocytes (PBLs), it is silenced in multiple leukemia cell lines. Overexpression of VSTM1-v1 in Jurkat cells inhibits cell growth (Li et al., 2015). In another study, high expression of VSTM1 in the U937 cell line, a model cell line for examining monocyte differentiation, decreased cell proliferation and increased apoptosis. Interestingly, VSTM1-depleted U937 cells showed NF-κB activation and increased inflammatory response (Wang et al., 2021).

Further investigations revealed that VSTM1-v2 increased the secretion of IL-17A and promoted Th17 cell differentiation (Guo et al., 2012). In addition, VSTM1-v2 has been identified as a potential biomarker for rheumatoid arthritis (RA) (Wang et al., 2016).

Extensive research has been conducted by the scientific community pertaining to VSTM1-v2, a glycoprotein that is released as a soluble form and possesses N-linked glycosylation. The presence of this protein in immune tissues suggests its involvement in immune responses. It is worth noting that scientists have identified VSTM1-v2 as a

potential cytokine, a type of protein that can have diverse effects on immune cells. Specifically, it has the ability to promote the differentiation and activation of Th17 cells, which play a crucial role in immune defense. Also, the impact of VSTM1-v2 on immune function is emphasized by its effect on the secretion of IL-17A, which is produced by CD4+ T cells. It is significant to take note that VSTM1-v2 deviates from another form of the VSTM1 protein, referred to as VSTM1-v1, in that it does not contain a transmembrane domain. (Guo et al., 2012).

A recent study discovered that individuals with RA had a heightened expression of VSTM1-v2 mRNA in PBMC samples compared to healthy subjects. The implications of these findings suggest that VSTM1-v2 may have the potential to serve as a useful biomarker for RA (Wang et al., 2016).

These findings hold important implications for subsequent research endeavors aimed at comprehending the roles executed by VSTM1-v2 and other constituents of the VSTM protein family in the immune system. Further exploration may aid in the creation of more efficacious therapies for autoimmune disorders such as RA.

1.3.2. VSTM2:

VSTM2 plays a critical role in regulating inflammation, cell death, and cytokine signaling. The 236 amino acids transmembrane protein VSTM2A has an extracellular region that includes an Ig domain and a signal peptide (Figure 4).

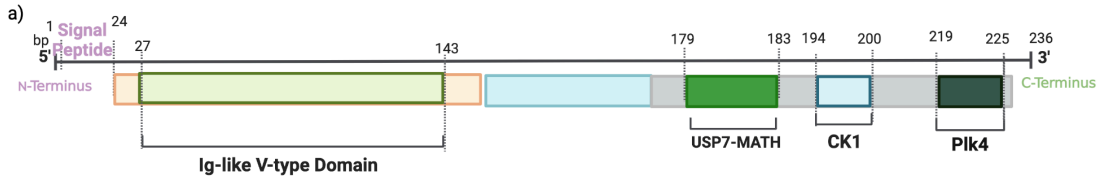

Figure 4. Structure of VSTM2. VSTM2A has an extracellular region that includes an Ig domain and a signal peptide.

VSTM2 isoforms, such as VSTM2A, VSTM2L, and VSTM2B, exhibit distinct characteristics and functions. VSTM2A, a transmembrane protein, has been implicated in adipogenesis, with its expression regulated by STAT3 during fat cell formation. On the other hand, VSTM2L is a soluble extracellular protein that modulates interleukin-4 (IL-4) signaling and shows associations with tumor infiltration, survival outcomes, and immune-related factors in various cancers. Additionally, VSTM2B has been identified as a potential biomarker for post-operative delirium and has differential expression in HPV-associated oropharyngeal squamous cell carcinoma. Further

research is needed to elucidate the precise mechanisms and clinical implications of these VSTM2 isoforms.

Researchers have discovered that VSTM2A is present during the formation of fat cells in the initial stages of adipogenesis, (Secco et al., 2017). The expression of VSTM2A is regulated by STAT3, which has been recognized as a transcription factor, and is expressed early on in *in vitro* fat cell formation (Al Dow et al., 2021). MII5, on the other hand, is posited to be responsible for errors in sperm maturation and has VSTM2A as one of its targets based on recent research (Dong et al., 2019). The repression of organoid and colon cancer cell line growth and the triggering of apoptotic signals in colorectal cancer cells have been established as the results of ectopic VSTM2A overexpression (Dong et al., 2019). Furthermore, the secretion of VSTM2A has been shown to hinder the Wnt pathway in colon cancer cells (Dong et al., 2019).

VSTM2L is a soluble extracellular protein that exhibits selective expression in the central nervous system. It has been characterized as a modulator of interleukin-4 (IL-4) signaling. Studies have revealed a correlation between VSTM2L expression and the infiltration of tumor cells, tumor mutation burden (TMB), and microsatellite instability. High expression of VSTM2L has been associated with lower survival in gastric cancer patients. In contrast, increased expression of VSTM2L has been found to increase disease-related survival in renal papillary cell carcinoma. Compared to healthy tissues, lower expression of VSTM2L has been observed in gastric and colon cancer tissues. Abnormal expression of VSTM2L has been linked to immune inhibitors, expression of major histocompatibility complex (MHC) molecules, and MSI in various cancers.

Zhang et al. analyzed the expression of VSTM2L mRNA in rectal cancer tissues. The results indicated that VSTM2L mRNA expression was higher in normal rectal tissues than in cancer tissues. Furthermore, they discovered that heightened VSTM2L expression was linked with patients having locally advanced rectal cancer (LARC) who failed to react to preoperative chemoradiotherapy (pCRT). Furthermore, high VSTM2L expression was correlated with shorter survival in research using data from the Gene Expression Omnibus (GEO) database. In the same study, organoid experiments from rectal cancer patients treated with pCRT revealed that increased VSTM2L expression lowered γ-H2AX expression (Zhang et al., 2022).

Through the IL-4 pathway, Liu et al. showed that augmented VSTM2L expression impeded apoptosis of cancer cells and fueled their proliferation (Liu et al., 2021). In

an *in silico* analysis to identify prognostic markers of ovarian cancer patients, they discovered 11 possible genes that may alter the patient's prognosis. Among these 11 genes, nine, including VSTM2L, were upregulated in high-risk patients with poor survival. This evidence implies that cancer progression significantly impacts VSTM2L and could potentially provide a therapeutic target for multiple cancers. However, further research is necessary to elucidate the underlying mechanisms by which VSTM2L modulates cancer development and progression. Therefore, monitoring VSTM2L expression levels in cancer patients may be beneficial to improve treatment outcomes.

VSTM2B (V-set and transmembrane domain-containing protein 2B) is categorized as a single-pass type-I integral membrane protein with an Ig-like V-type domain. The study on biomarker identification for the risk of post-operative delirium in elderly orthopedic patients with cerebrospinal fluid proteomic analysis indicated the potential use of VSTM2B as a biomarker for post-operative delirium (POD) diagnosis. However, further validation is necessary (Han et al ., 2020). Another study discovered that VSTM2B expression was high in patients with HPV-associated oropharyngeal squamous cell carcinoma (OPSCC) with differentially methylated regions (DMR). In another study, potential molecular-based 20-gene markers with high specificity in HPV-associated OPSCC, including VSTM2B, were identified (Ren et al., 2018).

1.3.3. VSTM3:

V-set and transmembrane domain-containing 3 (VSTM3, TIGIT) is essential for the recognition and signaling of antigens, as well as for the regulation of cytokine production and cell death. The VSTM family comprises various receptors, one such receptor is the cell immunoreceptor with immunoglobulin and ITIM domain (TIGIT, VSTM3). This receptor has been identified as an immunomodulatory receptor with potential as an immunotherapy target (Yu et al., 2009). The T-cell immunoreceptor with Ig and ITIM domain, known as TIGIT, is comprised of an extracellular domain consisting of an IgV region, a transmembrane domain, as well as an ITIM motif, and an Ig tail-tyrosine (ITT)-like motif (Figure 5) (Chauvin and Zarour, 2020).

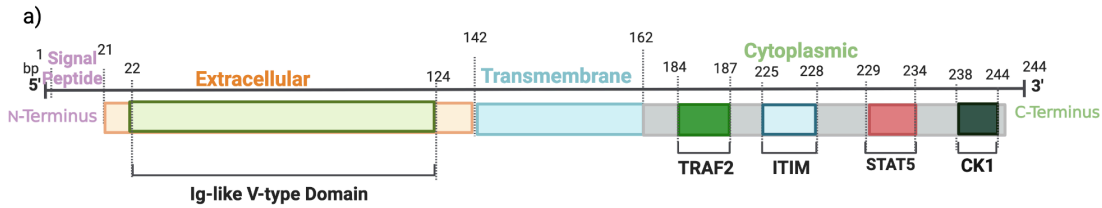

Figure 5. Structure ofVSTM3. TIGIT, is comprised of an extracellular domain consisting of an IgV region, a transmembrane domain, as well as an ITIM motif, and an Ig tail-tyrosine (ITT)-like motif.

The expression of TIGIT is mainly found on natural killer cells and T cells where it interacts with CD155 (PVR) and CD112 (PVRL2, nectin-2) ligands present on tumor cells and antigen-presenting cells, responsible for the inhibition of T and NK cell function.

Research findings indicate that TIGIT is prominently expressed in immune cells that are frequently utilized in cancer immunotherapeutic interventions (Harjunpää and Guillerey, 2020). The existing literature presents numerous plausible mechanisms for TIGIT-induced suppression of T and NK cells. A specific mechanism involves the lowered presentation of antigens and proinflammatory cytokines that manifests in CD155-expressing dendritic cells upon TIGIT and CD155 interaction (Yu et al., 2009). Additionally, it has been suggested that TIGIT disrupts DNAM-1 cis-homodimerization, preventing CD155-DNAM-1 interaction (Johnston et al., 2014). The capability of TIGIT to deliver inhibitory signals to NK and T cells through its cytoplasmic domain has been established, leading to its examination as a possible therapeutic agent for various autoimmune diseases (Stanietsky et al., 2013). Due to these potential mechanisms, TIGIT has generated substantial curiosity as an immunotherapeutic agent. As of now, 81 clinical trials are being conducted that cover a range of illnesses including cancer, immunodeficiency, diabetes, HIV, infections, and nervous system disorders (“Clinical Trials on TIGIT,” n.d.).

TIGIT's precise method of operation remains unexplained, yet six monoclonal antibodies that aim TIGIT as an immune checkpoint inhibitor have progressed toward clinical trials, nonetheless. TIGIT is considered one of the most significant members of the VSTM protein family due to its immune regulatory functions and potential as an immunotherapy target. The examination of TIGIT provides an understanding of its part in immunomodulation and its potential as a therapeutic agent.

1.3.4. VSTM4:

V-set and transmembrane domain-containing 4 (VSTM4) is involved in the regulation of inflammation and mediates cytokine signaling and T-cell activation.

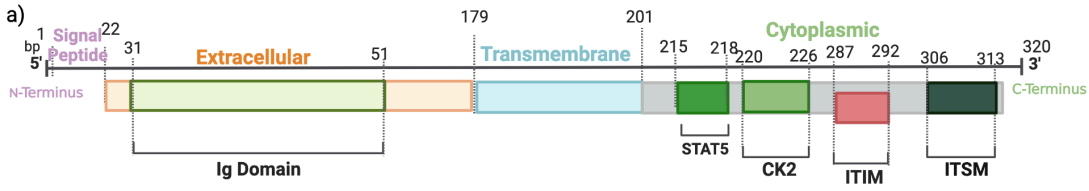

Figure 6. Structure of VSTM4. It has Ig domain in its extracellular region, a signal peptide, and a potential ITIM and ITSM motif in its cytoplasmic region.

VSTM4, a transmembrane protein of 320 amino acids, comprises the Ig domain in its extracellular region, a signal peptide, and a potential ITIM and ITSM motif in its cytoplasmic region (Figure 6). Peptide Lv, a fragment of VSTM4, enhances L-type voltage-gated calcium channels and possesses similar biological effects to vascular endothelial growth factor (VEGF) (Shi et al., 2012). The literature has limited studies on the function of VSTM4. Therefore, in our in silico investigations, we have identified motifs that may indicate the role of VSTM4.

There is a study by J. Wang et al. describing how the VSTM4-Fc construct significantly inhibits T cell production of inflammatory cytokines, including IFN-y, IL-2, and IL-17 in 2019 (Wang et al., 2019). In another study conducted by Mukai et al., it was found that macrophages expressed VSTM4 and its fragment, peptide Lv, but peptide Lv suppressed the production of TNF-α and IFN-y in macrophages (Mukai et al., 2021).

The ITIM motif contained within VSTM4's cytoplasmic region is highly unlikely to cause a decrease in T cell production of inflammatory cytokines, as stated by J. Wang *et al.*'s (2019) study and other immune functions (Wang et al., 2019). This suggested function may be vital for protein function, so further studies are required.

1.3.5. VSTM5:

VSTM5 is a highly conserved transmembrane protein (Figure 7) consisting of SLAM and Ig domains. VSTM5 has Ig domain, 2B4 and ITIM motifs in its extracellular region and potential tyrosine kinase binding sites in its cytoplasmic region. (Figure 8) (Lee et al., 2017)

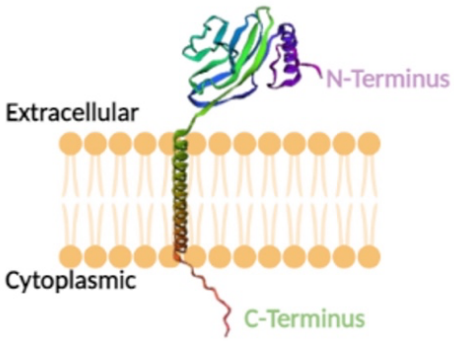

Figure 8. The membrane topology of VSTM5. The N-terminus is represented by purple, while the transmembrane region is indicated by the helix structure. The C-terminus is depicted in red.

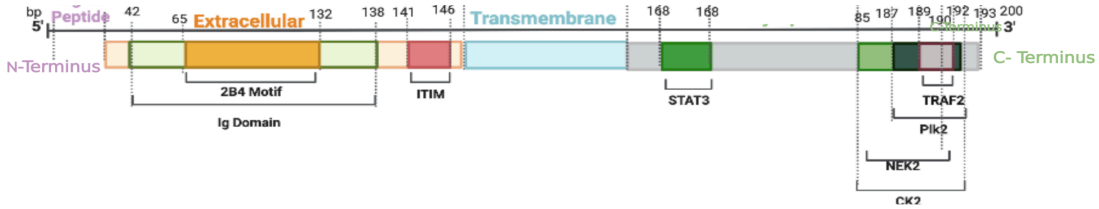

extracellular region and potential tyrosine kinase binding sites in its cytoplasmic region.

Despite the scarcity of studies on VSTM5, its conservation across species and primary expression in the central nervous system, followed by the stomach, kidneys, and small intestine, have been confirmed (Lee et al., 2016). In terms of its role in T cell microvilli formation as immunological synaptosomes, it has been suggested that VSTM5 has a minimal effect on the activation of cells. Nevertheless, it has been proven to possess four distinct N-glycosylation sites, vital in surface expression, and control neuronal morphology through F-actin, promoting synapse formation in neurons (Lee et al., 2016). Furthermore, VSTM5 has been shown to induce filopodial protrusions in the cell membrane, and it has been found that Cdc42 is critical to its function and can be activated by VSTM5.

One study conducted in 2016 (Zurit Levine, Galit Rotman, Liat Dassa, Ofer Levy,

Gad S. Cojocaru, Amir Toporik, Yossef Kliger, Andrew Pow, 2016) suggested that VSTM5 antibodies could be used to treat cancer, infectious diseases, and immune-related diseases. Immunohistochemical staining of VSTM5 has been observed to be negative in colon epithelial cells and positive in colon adenocarcinoma tumors and immune cells that infiltrate these tumors. Still, these results have been reported in many patients and quantitatively. In the same study, it was suggested that VSTM5 might have receptors in these cells, with the observation that VSTM5-ECD-Ig binds specifically to the human H9 T cell line in limited studies in T cells, but its receptor has not been identified.

More recently, a study of this protein with T cells obtained from mouse spleen has shown that VSTM5 significantly inhibits T cell division and decreases IL-2 production depending on the VSTM5 dose. In later studies, it was determined that VSTM5 expression also inhibits B cell responses, as well as T cell responses, and contributes to the anergy of T cells. Despite the limited research on VSTM5, its potential utilization in treating various illnesses and its role in immune system regulation make it a promising study area. Further inquiry in this sphere may uncover new and innovative therapies for a number of diseases.

The expression of the VSTM5 gene in colon cancer cell lines remains largely unexplored in the existing literature. However, through *in silico* studies, it has been found that the lung cancer cell line A549 exhibits the highest expression of VSTM5 (Expression Atlas, 2023). This suggests the need for further investigations to elucidate the role of VSTM5 in colon cancer and its potential implications for diagnosis and treatment.

The research extensively documents the involvement of V-set and transmembrane domain-containing 5 (VSTM5) in neural development and their ability to suppress cytotoxic T lymphocytes while impeding T cell proliferation. As a result, VSTMs are known to be critical components of the immune system, with each member possessing unique functionalities that are indispensable for the optimal operation of the system.
LncRNA regulates mRNA expression through competitive binding with miRNA and affects the function of mRNA. A recent study shows that long non-coding RNA of VSTM5 regulates ten miRNA's, which in turn dysregulates critical RNA's for cancer development and metastasis (e.g. TP53, MMP1, VEGF-A) or anti-tumor immune responses (i.e. FAS, STAT3, JUN, TRAF5), suggesting an alternative mechanism for VSTM5 associated regulatory pathways for cancer (Shaoxiong et al., 2022)

The VSTM gene family plays a crucial role in the modulation of immune pathways. Signal transmission and protein-protein interactions in VSTM proteins are facilitated by transmembrane domains, while ligand binding and the V-set domain are thereby facilitated. Antigen recognition, cytokine signaling, and T cells function on some of these proteins.

1.4. The Aim of the Study

In our conducted statistical analyses, we have determined that ***the disease-specific survival time of patients with CMS1 subgroup colon cancer, who exhibit high expression of the VSTM5 gene, is significantly longer than those with low VSTM5 expression*** (Figure 9).

Because of this observation, we have initiated our preliminary investigations to address the research question, "*What are the underlying mechanisms behind the extended survival of colon cancer patients with high VSTM5 expression?*"

The impact of VSTM5 expression on survival could be attributed to either a direct effect on cancer cells themselves, such as their growth rate, or interactions with the tumor microenvironment, or it may be dependent on the host's anti-tumor immune responses.

We have assessed that the first variable to be examined is the influence of VSTM5 expression on the growth rate of colon cancer cells.

Based on the result in Figure 9, approximately 50% of colon cancer patients with low VSTM5 expression remain alive at day 600, while over 90% of patients with high VSTM5 expression survive, we have postulated that the growth rate of colon adenocarcinoma cells, exhibiting high VSTM5 expression would be lower, compared to those with low VSTM5 expression. As a result, we have conducted our initial investigations to test the hypothesis that *the growth rate of colon adenocarcinoma cells is lower with high VSTM5 expression compared to adenocarcinoma cells with low*

VSTM5 expression.

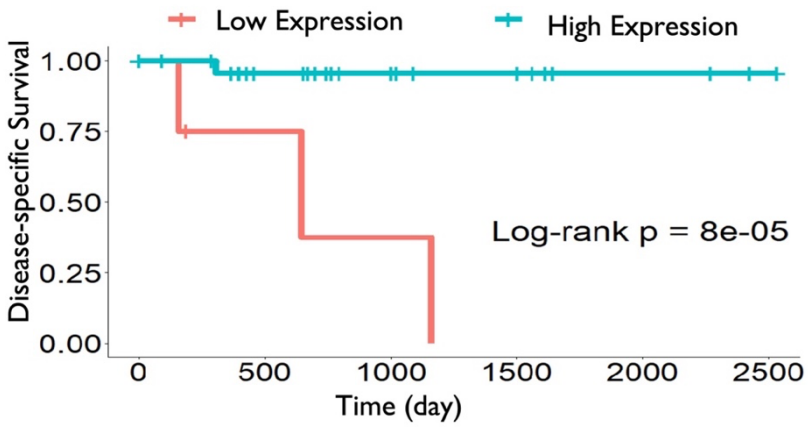

Figure 9. The VSTM5 protein expression is highly correlated with disease-specific survival of CMS1 colon cancer patients. Kaplan-Meier survival plot of disease-specific survival is depicted against time. The patient group with high AVSTM5 expression of CMS1 colon cancer shown with turquoise line. The patient group with low VSTM5

CHAPTER 2: METHODOLOGY

2.1.In silico Studies

2.1.1. ELM (Eukaryotic Linear Motif) & ExPASy (Expert Protein Analysis System)

We utilized the ELM (Eukaryotic Linear Motif) and ExPASy (Expert Protein Analysis System) databases to generate gene motifs and domains for VSTM family proteins (Figure 3-7). The ELM database serves as a comprehensive repository of short linear motifs identified in eukaryotic proteins, offering valuable insights into potential protein-protein interactions. On the other hand, ExPASy is a vast database encompassing protein sequence information and functional annotations, facilitating the discovery and evaluation of protein domains. We have identified functional domains and motifs for VSTM1, VSTM2, VSTM3, VSTM4 and VSTM5 through these resources. The outcomes of our analysis were visualized using Biorender software (BioRender.com).

2.1.2. Protein – Protein Docking (HADDOCK)

In order to gain insight on the yet unidentified potential receptors of VSTM5, we employed protein-protein docking. The protein-protein docking analyses involving different immune receptors and the VSTM protein family were conducted using the HADDOCK version 2.4 online tool. To initiate the process, the PDB files of the VSTM protein family (PDB IDs: AF-A8MXK1-F1) and the immune receptors (NK2DL2 (PDB ID: 2M2D), Fc-Gamma Receptor III (PDB ID: 1E4J), NK2DL4 (PDB ID: 3BDW), KIR2DS2 (PDB ID: 1P6F), NKG2A (PDB ID: 3NOI), NKp46 (PDB ID: 3WYR), NKp30 (PDB ID: 2Q87), CD158d (PDB ID: AF_AFQ9NZN1F1), CD300 (PDB ID: 6AED), IL1R8 (PDB ID: AF_AFA0A5K1VDZ0F1), ILT2_LIR1 (PDB ID: 2DL2), KIR2DL1 (PDB ID: 2M2D), KIR2DL2 (PDB ID: 5F71), PD-1 (PDB ID: AF_AFP40200F1), TIM3 (PDB ID: AF_AFQ5U334F1) were obtained from the Protein Data Bank (PDB). The protein structures used for the docking simulation in HADDOCK were prepared by applying modifications using the Dock Prep module of UCSF Chimera software version 1.16. These modifications involved the removal of ligands, water molecules, and heteroatoms, as well as the addition of partial charges and hydrogens. Furthermore, the side chains were replaced with the Dunbrack 2010 rotamer library to optimize their conformation. These steps were crucial to ensure that

the protein structures were properly prepared for accurate docking simulations in HADDOCK, allowing for the analysis of protein-protein interactions and potential binding sites.

To identify the interacting amino acids within the proteins, the SPPIDER II algorithm was employed. The identified interacting residues were used as an input when submitting the samples to the HADDOCK tool. The resulting outputs were analyzed based on the HADDOCK score and Z-score. The HADDOCK score and Z-score are numerical measures used to assess the quality and reliability of protein-protein docking models generated by the HADDOCK software. The HADDOCK score is an energy-based metric that evaluates the overall quality of the docked complex, with lower scores indicating more favorable binding conformations. On the other hand, the Z-score provides a statistical comparison of the HADDOCK score to a reference dataset, indicating the deviation from the mean score and providing a measure of the model's relative quality compared to other docking results. A lower HADDOCK score and a higher Z-score suggest more reliable and accurate docking predictions, but it is essential to consider these scores alongside visual inspection and experimental validation to ensure the robustness of the results in a given system.

2.2.In vitro studies

2.2.1. Cell culture

The utilization of cell lines in biological research is crucial for investigating various biological processes and their reactions under different experimental conditions. The utilization of two frequently employed cell lines, namely A549 human lung epithelial and LoVo human colon adenocarcinoma, entails culturing them in a specific medium type known as Ham’s F-12K, which harbors a high concentration of glucose (3.5g/l). To ensure the cells' growth and sustenance, the medium is further supplemented with 10% Fetal Bovine Serum (FBS) and 1% Penicillin-Streptomycin, providing the necessary growth hormones and antibiotics.

CCD18-Co, a well-known healthy colon epithelium model in scientific literature, has become a frequently employed control in various research studies (González-Sarrías et al., 2022; Ishak et al., 2023). Its use enables comparative analyses and provides a reference point for evaluating experimental outcomes in the context of normal colon epithelial cells. CCD18-Co human colon epithelial cell line, on the other hand, is preserved in a distinct medium referred to as DMEM. It has 10% FBS and 1%

Penicillin-Streptomycin. On the other hand, HCT116 and HT29 human colon adenocarcinoma cell lines are maintained in McCoy's 5A medium supplemented with 10% FBS and 1% Penicillin-Streptomycin. All cell lines were cultured in T25 or T75 cell culture flasks in an incubator with a 5% CO2 atmosphere and at 37°C.

The A549 cell line is selected for this study due to its high expression of VSTM5 through Expression Atlas (EDI, n.d). CCD18-Co, defined as a normal colon epithelial tissue cell line, was used as a healthy colon tissue sample for comparison. In contrast, HCT116, HT29, and LoVo cell lines were identified as CMS-1 group colon cancer cell lines and were utilized as experimental groups in this study.

2.2.1.1. Subculturing of Cells

The technique of collecting cells from a culture and transferring them to one or more culture containers with fresh growth media is known as passage or subculturing. Before passaging, cells were examined under a microscope (Olympus, CKX53SE) to confirm their confluency. Cells were not allowed to culture above 80% confluency. The laminar flow cabinet surfaces were disinfected with 70% ethanol before passaging. Every material taken into the cabinet was disinfected with 70% ethanol unless previously sterilized. Before use, the Trypsin-EDTA solution (0.25%, Gibco) and culture medium were equilibrated to 37ºC from 4°C storage in a water bath (Mipro, MCS30). Cells grown in T75 cell culture flasks were placed in the laminar cabinet, and the medium was aspirated. The surface of the cell culture flask was washed with 8 mL of 1X phosphate-buffered saline (PBS), and the PBS was also removed.

Then, 2 mL of Trypsin-EDTA solution was added to the T-75 flask. The flask containing trypsin-EDTA solution was incubated for 5 minutes in the incubator. After incubation, the cells were examined under a microscope, and further incubated if necessary until they become rounded and mostly detached from the flask surface. The flask was gently tapped on the base and sides to detach the cells from the flask surface entirely. The flask was then transferred to the laminar flow cabinet, and 3 mL of growth medium was added to inactivate the Trypsin-EDTA solution. The cell solution was transferred to 15 mL falcon tubes. The falcon tubes were centrifuged at 500 g for 5 minutes with refrigerated centrifuge (Hettich Rotina 380R). After centrifugation, the supernatant in the falcon tubes was discarded, and the pellet at the bottom of the tube was resuspended in 1 mL of cell medium. 250 µL of the cell solution was transferred

to cell culture flasks containing 10 mL of fresh medium and placed in the incubator. The passaging process was repeated as necessary for different cell lines.

2.2.1.2. Cell Counting

Cultured cells were counted using a hemocytometer to ensure a consistent number of cells were used for each protocol. The cells were separated from the bottom of the flask using Trypsinization and collected in a falcon tubes. The tube was centrifuged for 5 minutes at 500 g value, and the supernatant was removed from the centrifuged falcon tube. The pellet was then dissolved in 1 mL of medium, and 50 µL aliquots of the suspended cell solution were transferred to 1.5 mL microcentrifuge tubes.

To count the cells, 90 µL of Trypan-blue was added to one well of a 96-well plate, followed by 10 µL of cell solution to make a 1:10 dilution. Using a microscope, the cells werecounted from 10 µL cell solution on the hemocytometer. With intact membrane integrity, live cells appeared bright white and did not absorb the blue dye.

The cells were counted in 5 squares on the hemocytometer, and the number of cells in 1 mL was calculated using the formula (1) below.

$$Number\ of\ Cell/mL = \frac{Number\ of\ counted\ cells}{5} \times\ Dilution\ factor\ \times\ 10^4 \quad (1)$$

The suspended cells were then diluted to the desired cell count and used for further experimentation, such as creating cell cultures, cell stocks, or pellets.

2.2.1.3. Cell cryopreservation and harvesting

The cryopreservation of cells was conducted under sterile conditions in a laminar flow cabinet. The procedure began by removing the medium from the 75T cell culture flask and washing it with 8 mL of 1X PBS. Subsequently, 2 mL of Trypsin-EDTA solution was added to the flask, and the cells were incubated at 37°C for 5 minutes. The detached cells were gently separated by tapping the right and left sides of the flask, and the flask was taken to the laminar flow cabinet. Next, 3 mL of growth medium was added to 15 mL of a flask and centrifuged at 500 g for 5 minutes. The supernatant was discarded, and the pellet was thawed in 1 mL of freezer medium. Cell counting was performed following the method outlined in the cell counting procedure. The cell solution was then diluted to $1x10^6$ cells, and 1 mL of the solution was transferred to

cryovial tubes. These tubes were kept at -20°C for 3 hours and then stored at -80°C overnight. The next day, the cryovial tubes were transferred to a liquid nitrogen tank for long-term storage to prevent loss of cell viability. Cells not to be cryopreserved were transferred to 2 mL Eppendorf tubes at $1x10^6$ cell count, the Eppendorf tubes were centrifuged at 2850 rpm for 5 minutes, and the supernatant was removed. The pellet remaining in the Eppendorf tubes were stored at - 80ºC for further studies. This cryopreservation method is a reliable means of preserving cells for future use. The use of liquid nitrogen ensures that the cells remain viable and can be used for future experiments or studies, as human cancer cell lines rapidly lose their viability within 6 months to a year when stored in -80ºC

2.2.1.4. G418 Antibiotic Killing Curve with MTT

An antibiotic killing curve is an experimental procedure where varying concentrations of a specific antibiotic, in this case, G418, are applied to cell cultures, such as LoVo cell lines, to determine the optimal antibiotic dosage. G418 serves as the recommended antibiotic for selecting cells carrying the pcDNA3-EGFP plasmid, which includes a G418 resistance gene. The purpose of conducting this antibiotic killing curve is to identify the precise G418 concentration necessary to selectively eliminate untransfected cells while allowing those transfected with the pcDNA3-EGFP 3 plasmid to survive. By employing the appropriate antibiotic dosage, the survival of only those cells harboring the pcDNA3-EGFP 3 plasmid is ensured, thereby affirming the effectiveness of the transfection and selection procedures. For this purpose, lethal dose of G418 for a minimum of over 90% parental cell death needs to be determined within the selection time period.

LoVo cells were cultured, harvested, and quantified following the procedures outlined in sections 1.2 and 1.3. Subsequently, LoVo cells were seeded into a 96-well cell culture plate at a density of 6000 cells per well in 100 μL of Ham's F12 medium. To facilitate cell adhesion and promote cell health, the plates were then incubated for 24 hours at 37°C with 5% CO2. After this incubation period, the cellular morphology and density were assessed via microscopy. The culture medium was then aspirated from the 96-well plate, and it was replaced with Ham's F12 medium supplemented with G418 at 12 distinct concentrations spanning the range of 0-2 mg/mL. Cells were subsequently subjected to incubation in the antibiotic-containing medium until the optimal antibiotic concentration was identified, resulting in the complete elimination

of 100% of cells within a period ranging from 2 to 15 days from the onset of the selection process. Every 3-day interval, the culture medium was renewed with fresh medium containing antibiotics within the same concentration range.

In the antibiotic kill curve protocol, the dose of G418 at which 100% cell death was observed in LoVo cells at 3 days was determined. Subsequently, the MTT cell viability assay was employed to assess the death rate of the cells and calculate the LD50 and LD90 doses. The MTT assay, based on the reduction of the yellow MTT tetrazolium salt into purple formazan crystals by metabolically active cells, provided a reliable means of quantifying cell viability in response to varying G418 concentrations, enabling a comprehensive evaluation of the cytotoxic effects of the antibiotic on the LoVo cell line.

Various antibiotic concentrations were introduced into the cell culture medium, as elaborated in Section 2.2.1.4. Following a 3-day incubation period, 15 µL of MTT solution was meticulously dispensed into each well, followed by a 4-hour incubation period. Subsequent to this incubation, the MTT solution was carefully aspirated, and the resultant formazan crystals were solubilized in 100 µL of dimethyl sulfoxide (DMSO). Incubation at room temperature in the absence of light was sustained for 30 minutes to facilitate formazan dissolution, and the optical density (OD) was quantified at wavelengths of 570 nm and 620 nm.

2.2.2. RNA Isolation

RNA isolation was conducted using the MN-NucleoSpin RNA Mini Kit (#Cat no: 740955.50) from Macherey-Nagel, Germany, according to the manufacturer's instructions. Following isolation, the concentrations and purity of RNA samples were assessed using a Nanodrop instrument (Cat. No: MN-913A) (MaestroNano, Maestrogen, Taiwan) by measuring the absorbance ratio at 260/280 nm.

The cells were pelleted to contain $1x10^6$ cells, as described in section 2.1.4. To lyse the cells, 350 µL of RA1 solution and 3.5 µL of ß-mercaptoethanol (ß-ME) were added to the pellet and vortexed. The cell lysate was then transferred to an Eppendorf containing a NucleoSpin filter to complete cell lysis with centrifugal force. The mixture was centrifuged at 11,000g for 1 minute, and the NucleoSpin filter was discarded. Next, 350 µL of 70% ethanol was added to the Eppendorf containing the lysate, and the lysate was homogenized by pipetting. A NucleoSpin RNA Column was

placed in the Eppendorf, and the lysate was loaded into the column and centrifuged at 11,000g for 30 seconds. The column was then placed in a clean Eppendorf.

350 µL of Membrane Desalting Buffer (MDB) was added to the column, then centrifuged at 11,000g for 1 minute to desalt the membrane. A DNase reaction mixture was prepared to digest DNA by adding 90 µL of Reaction Buffer for rDNAse to 10 µL of reconstituted rDNase. The DNase reaction mixture was added to the column and incubated for 15 minutes at room temperature. After incubation, 200 µL of Buffer RAW2 was added to the column and centrifuged at 11,000g for 30 seconds to inactivate rDNAse. The column was then placed in a new Eppendorf tube.

To elute RNA, 600 µL of Buffer RA3 was added to the column and centrifuged at 11,000g for 30 seconds. The flowthrough was removed, and the column was placed back into the same Eppendorf tube. 250 µL of Buffer RA3 was added to the column to dry the membrane completely and centrifuged at 11,000g for 2 minutes. The column was then placed in a new Eppendorf tube.

To separate the RNA from the column, 60 µL of RNase-free H2O was added to the column and centrifuged at 11,000g for 1 minute. The column was discarded, and the Eppendorf was labeled correctly. The concentration and purity of the RNA samples were measured using a Nanodrop (MaestroGen, MaestroNano). Background was measured with a blank was created using 2 µL of RNase-free H_2O or the solution used for dissolving such as TE buffer, and at least three consistent measurements were taken after measuring 2 µL of RNA samples.

2.2.3. cDNA Synthesis

Various concentrations of RNA were extracted from each cell line. The OneScript Plus cDNA Synthesis Kit (Applied Biological Materials Inc. Canada Catalog Number: G236), was utilized to synthesize cDNA from the RNA samples using 1 µg following the manufacturer's protocol outlined below:

All the procedures were carried out on ice.

4 µL of 5X RT buffer, 1 µL of dNTP, 1 µL of primers, 1 ug of total RNA, and 1 µL of OneScript Plus RTase were added to a final volume of 20 µL with the addition of nuclease-free H_2O.

The solution was gently mixed and incubated at 55°C for 15 minutes.

Following the incubation, the reaction was terminated by incubating at 85°C for 5

minutes and then placing the samples on ice. The generated cDNAs were stored at -20°C.

2.2.4. PCR & qPCR and Agarose Gel Electrophoresis

2.2.4.1. qPCR

The RT-qPCR reaction was conducted in 96-well reaction plates using RealQ Plus 2x Master Mix Green (Ampliqon, Denmark Cat.no: A323402), which contains all the necessary components for the reaction, including enzymes, nucleotides, and buffer. All reactions were performed in at least two replicates with a final volume of 20 µL, although the PCR reaction works with 10µL efficiently All experimental reactions were conducted in accordance with the specifications outlined in Table 1.

Table 1. Components of qPCR

Component	Volume per reaction
RealQ Plus 2x Master Mix	10 mL
Forward Primer (4 mM)	2 mL
Reverse Primer (4 mM)	2 mL
Template DNA (100 ng)	4 mL
PCR-grade H2O	2 mL

Primer sequences were designed using the Benchling online tool (Table 2) and subsequently verified through the Genome Data Viewer and Primer Blast tools available at the National Center for Biotechnology Information (NCBI). Primers were synthesized by Sentebiolab (Ankara,Turkey).

Table 2. Primer Sequences used qPCR

Primer	Sequence	Predicted Product Size
VSTM5 Forward	5'AGGACTCTTCGCCCTCTGCCTG3'	146 bp
VSTM5 Reverse	5'TGGTGGGCACTCCATGACAGGA3'	
β-actin Forward	5'AAGGATTCCTATGTGGGCGAC3'	283 bp
β-actin Reverse	5'CGTACAGGGATAGCACAGCC3'	
18S rRNA Forward	5'CGGCTACCACATCCAAGGAA3'	186 bp
18S rRNA Reverse	5' GCTGGAATTACCGCGGCTGC 3'	

Real-time PCR reactions were performed using the CFX Connect Real-Time PCR Detection System (BIORAD, California USA), following the protocol outlined in Table 3.

Table 3. Three-step qPCR Protocol for VSTM5

Analysis Mode	Number of cycles	Temperature (°C)	Hold Time (mm: ss)
Enzyme activation	1	95°C	15:00
Denaturation		95°C	00:30
Annealing	40	55°C (var.)	00:30
Extension		72°C	00:30 (variable)
Melt Curve	1	65°C to 95°C	0:05 per 1°C

2.2.4.2. High Fidelity PCR:

The PCR reaction was conducted in 96-well reaction plates using Phusion™ High-Fidelity DNA Polymerase (Thermo Fisher, USA Cat. no: F530S), which contained all the necessary components, including enzymes, nucleotides, and buffer. The primers were designed using the Benchling online tool (Table 4) and subsequently validated for primer sequence using the Genome Data Viewer and Primer-BLAST at the National Center for Biotechnology Information (NCBI). Sentebiolab (Ankara,Turkey) synthesized the primer sequences. The primers were diluted in TE buffer according to the manufacturer's recommendations to a final concentration of 100 µM and stored at -20°C until ready for use. Each reaction was performed in a final volume of 50 µL and

replicated at least twice. For the preparation of each reaction, 10 µL of 5X Phusion HF Buffer, 1 µL of the primer pair, 1.5 µL of DMSO, and PCR grade H_2O were added to achieve a final volume of 50 µL for each 500 ng of cDNA. The PCR reactions were carried out using a Thermal Cycler (Applied Biosystems, USA). The PCR protocol involved an initial denaturation step at 98°C for 30 seconds, followed by 42 cycles of denaturation at 98°C for 10 seconds, annealing at 55°C for 15 seconds, and extension at 72°C for 90 seconds.

Table 4.Primer Sequences used Hi-Fi PCR

Primer	**Sequence**	**Predicted Product Size**
VSTM5 Forward	5'CGATCCTGAAGAGAGAAGGCTGCATA3'	2909 bp
VSTM5 Reverse	5'GAGCTCTAAACCTCAGGCTCTGCATT3'	
18S rRNA Forward	5'CGGCTACCACATCCAAGGAA3'	186 bp
18S rRNA Reverse	5' GCTGGAATTACCGCGGCTGC 3'	

2.2.4.3. Touchdown PCR:

The Taq DNA Polymerase 2x Master Mix (Ampliqon, Denmark Cat.no: A140301) was utilized to perform the touchdown PCR protocol. The master mix has all the necessary ingredients including the Taq DNA polymerase, $MgCl_2$, and dNTPs. The final volume of each PCR tube was 50 µL, and all experiments were carried out in duplicates. Repetition of the experiment on three different days was done to ensure reproducibility. The experimental reactions were prepared based on the details provided in Table 5. The primer sequences were designed using the Benchling online tool and then verified for their accuracy by aligning them with the genomic data using the Genome Data Viewer and Primer BLAST tools provided by the National Center for Biotechnology Information (NCBI). The primer sequences were synthesized by Sentebiolab (Ankara,Turkey).

Table 5. Components of Touchdown PCR

Component	Volume per reaction
Taq 2x Master Mix	25 µL
Forward Primer (10 µM)	1 µL
Reverse Primer (10 µM)	1 µL
Template DNA (100 ng)	8 µL
PCR-grade H_2O	15 µL

Table 6. Primer Sequences used Touchdown PCR

Primer	**Sequence**	**Predicted Product Size**
VSTM5 Forward	5'GGATCCAATATGAGGCCTCTGCCA3'	603 bp
VSTM5 Reverse	5'CTCGAGCTAACACTCAACATCTTCCAGC3'	

2.2.4.4. PCR

The Taq DNA Polymerase 2x Master Mix (Ampliqon, Denmark, Catalog number: A140301) was employed to execute the PCR protocol. This master mix encompasses all essential components, including Taq DNA polymerase, MgCl2, and dNTPs. Each PCR tube was prepared to a final volume of 50 µL, and all experiments were conducted in duplicate. To ensure reproducibility, the experiment was repeated on three distinct days. The experimental reactions were prepared in accordance with the parameters specified in Table 5, and the High Fidelity PCR product generated in section 2.4.4.2 was subsequently isolated and employed as the template DNA. Primer sequences were designed using the Benchling online tool and subsequently validated for their accuracy by aligning them with genomic data utilizing the Genome Data Viewer and Primer BLAST tools provided by the National Center for Biotechnology Information (NCBI). The primer sequences were synthesized by Sentebiolab (Ankara, Turkey).

2.2.4.5. Agarose Gel Electrophoresis

The accuracy of PCR and qPCR products was assessed using agarose gel electrophoresis. A 2% agarose gel was prepared, and the samples were electrophoresed for 1.5 hours. To prepare the agarose gel, 2 grams of agarose were dissolved in 100 mL of 1X TAE buffer for a 2% gel and heated in a microwave while stirring occasionally until homogenous. Once the agarose was warmed, 6 µL of Et-Br or SYBR Safe dye was added and mixed. The agarose was then poured into an electrophoresis tank, and the tank's comb was placed and left to solidify. After the agarose gel was solidified, 1X TAE buffer was poured onto it, the comb was gently removed without damaging the gel, and 5 µL of 1kb Plus Opti-DNA Marker (Applied Biological Materials Inc. (ABM), Canada Cat.no: G248) was added to the first and last wells. To load the PCR sample, 10 µL of the sample was mixed with 2 µL of 5x DNA Loading Buffer Red (Ampliqon, Denmark Cat. No: A608104). Ten microliters of the sample per well were loaded and run at 100 Volts for 1.5 hours. The resulting bands were visualized using a Fusion Solo S transilluminator (Vilber, Germany) at the end of the electrophoresis run.

2.2.4.6. PCR Product Purification from Agarose Gel

The NucleoSpin Gel and PCR Clean-up Kit (MN, Germany Cat.no: 740609.50), was employed for the purification of the products obtained from High Fidelity PCR and touchdown PCR reactions. It is critical to purify the PCR-amplified product for subsequent applications such as restriction digestion and molecular cloning. The purification process was initiated by excising agarose gel bands that contained the desired DNA fragments utilizing a scalpel, and the precise weight of the gel was determined. Every 100 mg of the gel was supplemented with 200 µL of NTI Buffer in a microcentrifuge tube and incubated at 50°C with intermittent vortexing to guarantee complete melting of the agarose gels. The resulting melted agarose suspension was then transferred to a NucleoSpin Gel and PCR Clean-up Column placed in a 2 mL Collection Tube. After centrifugation at 11,000g for 30 seconds, the supernatant was carefully removed. This process was repeated until the entire suspension was loaded into the column. To cleanse the silica membrane and eliminate any impurities, 700 µL of NT3 Buffer was introduced to the column, followed by centrifugation at 11,000g for 30 seconds. The washing step was repeated to prevent the transfer of chaotropic

salt for a high A260/A230 value. Subsequently, the silica membrane was centrifuged at 11,000g for 1 minute to eliminate residual NT3 buffer. The collection tube containing the column was subjected to incubation at 70°C for 5 minutes to vaporize any residual ethanol. Ultimately, the column was transferred to a new 1.5 mL centrifuge tube, and 30 µL of Buffer NE was introduced. The mixture was incubated at room temperature for 5 minutes and subsequently centrifuged at 11,000g for 1 minute. After centrifugation, the purified samples were appropriately labeled and stored at -20°C for future use.

2.2.5. Molecular Cloning

2.2.5.1. Heat Shock Transformation

To initiate the transformation process, competent DH5α cells were retrieved from -80°C storage and thawed on ice. Purified plasmid DNA was combined with the competent cells, and the resulting mixture was incubated on ice for 30 minutes. Subsequently, the tube containing the mixture was subjected to a heat shock at 42°C for 45 seconds, followed by an immediate return to an ice bath for 2 minutes.

To facilitate the recovery and growth of the transformed cells, 80 µL of SOC medium was added to the tube. The culture was then incubated at 37°C for 1 hour in an orbital shaker. After incubation, the culture was spread onto a selective medium containing the appropriate antibiotic (LB Agar-Amp). The plates were subsequently incubated overnight at 37°C to allow for colony formations.

2.2.5.2. Plasmid Isolation

After incubation, a single colony was selected and transferred to a medium supplemented with the appropriate antibiotic (LB-Amp). Following a 16-hour incubation period with shaking at 37ºC, plasmid isolation was performed using the GeneJet Plasmid MiniPrep (Thermo Fisher, USA Cat. no: K0502) kit.

To initiate the process of plasmid isolation, a sterile eppendorf tube was utilized to transfer 2 mL of LB medium containing the bacteria that carried the plasmid. After this, the tube was centrifuged at 6800g for 2 minutes to help collect the bacterial pellet that had settled at the bottom. To guarantee the proper mixing of the pellet, 250 µL of Resuspension Solution was added to the eppendorf tube, effectively resuspending the pellet. Afterwards, 250 µL of Lysis Solution was added into the tube and the contents

were gently mixed until no visible cell clumps are present. To stabilize the lysed sample, 350 µL of Neutralization Solution was added, and the tube was inverted four times to guarantee complete mixing. Next the eppendorf tube was centrifuged to, at 12000g for 5 minutes, thereby allowing the supernatant to effectively dissociate from the remaining mixture. With the utmost care, the supernatant was then transferred to a GeneJET spin column. At a speed of 12000g, the column underwent a 1 min. centrifugation to eliminate any remaining liquid before being returned to the collection tube.

A volume of 500 µL of Wash Solution was introduced into the column for the purpose of purifying the plasmid. The column was then subjected to centrifugation at a force of 12000g for a duration of 1 minute. The resulting supernatant was discarded, and the washing process was repeated. Subsequently, the GeneJET spin column was carefully transferred to a sterile 1.5 mL eppendorf tube. Adding Elution Buffer to the column followed by incubation for 5 minutes at room temperature resulted in the elution of the isolated plasmid. The tube was then subjected to centrifugation at a force of 12000g for a duration of 2 minutes. The column was then removed, leaving the purified plasmid in the eppendorf tube. Finally, the isolated plasmid was stored at a temperature of -20°C until its subsequent use.

After the plasmids were isolated, their concentrations were evaluated using a Nanodrop instrument obtained from MaestroNano (Maestrogen, Taiwan Catalog Number: MN-913A) to facilitate the development of the restriction protocol. The HindIII (Catalog Number: FD0504) and BgIII (Catalog Number: FD0084) enzymes from Thermo Fisher (USA) were used to enzymatically digest the isolated plasmids according to the manufacturer's instructions.

2.2.5.3. Restriction Enzyme Digestion

Molecular cloning, a cornerstone of molecular biology, enables precise DNA manipulation and replication. In our study, we employed HindIII and BglIII restriction enzymes to selectively cleave the pcDNA3-EGFP vector and the VSTM5 CDS PCR product, facilitating the creation of compatible "sticky ends" for efficient ligation. These enzymes target specific recognition sites, as exemplified by HindIII (A/AGCTT) and BglII (A/GATCT) in our work. Moreover, the enzymatic cleavage process enhances ligation efficiency by aligning the sticky ends between the vector and DNA insert seamlessly.

Restriction endonucleases (RE) exhibit remarkable specificity, recognizing and cleaving specific DNA sequences. RE enzyme performance is influenced by factors like DNA substrate quantity and optimal cleavage temperature, typically at 37ºC. Our research meticulously applied this established methodology to insert the VSTM5 CDS PCR product into the pcDNA3-EGFP 3 vector, yielding recombinant DNA with exceptional precision and reliability.

In this thesis, we meticulously apply this well-established methodology to insert the VSTM5 CDS PCR product into the pcDNA3-EGFP 3 vector, obtaining recombinant DNA with exceptional sensitivity and reliability.

Reaction mixtures, comprising HindIII and BglII restriction enzymes, were prepared and outlined in Table 7.

Digestion reactions were meticulously prepared according to the specifications outlined in Table 7. The reaction mixtures were gently mixed and subjected to centrifugation. Incubation followed, first at 37°C for a duration of 30 minutes, and subsequently at 80°C for 10 minutes to halt the enzymatic reactions effectively.

Subsequently, the reaction products, including plasmid samples and 1% VSTM5 samples, were loaded onto 2% agarose gel matrices, following the procedures detailed in Section 2.2.4.4. Gel electrophoresis using agarose was conducted to assess the resulting DNA fragments.

Post-electrophoresis, the DNA products were extracted from the agarose gel in accordance with the methodology expounded in Section 2.2.4.6 and their respective concentrations were quantified utilizing a nanodrop spectrophotometer.

Table 7. Restriction Enzyme Digestion Protocols

Components	Plasmid Digest (HindIII)	VSTM5 Digest (HindIII)	Plasmid Digest (BgIII)	VSTM5 Digest (BgIII)	Plasmid Double Digest	VSTM5 Double Digest
Water (uL)	15.0	17.0	15.0	17.0	13.5	12.5
FastDigest Buffer Green (µL)	2.0	2.0	2.0	2.0	2.0	2.0
Plasmid DNA (µg)	1.0	-	1.0	-	1.0	-
PCR Product (ng)	-	0.2	-	0.2	-	0.2
HindIII (µL)	1.0	1.0	-	-	1.0	1.0
BgIII (µL)	-	-	1.0	1.0	2.0	2.0
Final Volume (µL)	20.0	30.0	20.0	30.0	20.0	30.0

2.2.5.4. Phosphorylation and Ligation

In molecular biology research, ligation and phosphorylation are fundamental techniques used to manipulate and join DNA fragments. Phosphorylation involves the addition of phosphate groups to DNA ends, while ligation is the process of covalently linking these modified DNA fragments together. These techniques are invaluable for tasks such as cloning, vector construction, and the creation of recombinant DNA molecules. Phosphorylation reaction mixture was performed as given in the Table 8 Ligation reaction mixture is given Table 9.

Table 8. Components and Protocol of Phosphorylation

Components	**Amount for Plasmid DNA**	**Amount for Insert DNA**
Plasmid DNA (360 ng/µL)	2.30 µL	-
Insert DNA (103 ng/µL)	-	8 µL
10X T4 Polynucleotide Kinase	2.5 µL	2.5 µL
T4 Polynucleotide Kinase	1 µL	1 µL
ATP (Adenosine triphosphate)	2.5 µL	2.5 µL
Nuclease-free water	16.7 µL	11 µL
Protocol		
Incubation Temperature	37°C	
Incubation Time	10 minutes	
Heat Inactivation	65°C for 10 minutes	

Table 9. Components and Protocols of Ligation

Components	**Amounts**
Plasmid DNA (360 ng/µL)	5.56 µL
Insert DNA (103 ng/µL)	6.81 µL
10X T4 DNA Ligase Buffer	2 µL
T4 DNA Ligase	1.5 µL
Nuclease-free water	5.38 µL
Protocol:	
Incubation Temperature	22°C
Incubation Time	10 minutes
Heat Inactivation	65°C for 10 minutes

Following the ligation process, competent DH5α bacteria were transformed with the ligation product, specifically the VSTM5^{+}pcDNA3-EGFP 3 plasmid. Subsequently, colonies were selected after transformation using antibiotics, and the plasmids were subsequently isolated as outlined in sections 2.2.5.1 and 2.2.5.2. Following the

isolation of plasmids in accordance with the established protocol, a PCR was conducted using CDS primers, as detailed in section 2.2.4.4. The isolated plasmids served as the template DNA for this procedure.

2.2.5.5. Transfection

Electroporation is a technique used to introduce DNA, RNA, or other molecules into cells by exposing them to an electric field. It is widely applied in gene transfer, drug delivery, and genetic modification. While versatile and effective for a variety of cell types, it can potentially cause cell damage and is less suitable for in vivo applications due to the difficulty of applying electric fields within living organisms. Optimization is crucial for consistent results, as transfection efficiency may vary between conditions and cell types.

For electroporation of LoVo cells, a culture with a concentration of $1x10^6$ cells/mL was prepared, a plasmid solution with a concentration of 20 µg/mL was obtained. Electroporation was carried out using a voltage of 150 V with a single pulse, and PBS served as the electroporation buffer. Following electroporation, the cells were promptly transferred back to a culture dish containing cell culture medium and subsequently incubated under standard conditions. Subsequent to incubation, the cells were monitored for gene expression or any desired plasmid-induced effects. This protocol provides a comprehensive framework for the successful electroporation of LoVo cells with the pcDNA3-EGFP plasmid, offering detailed guidelines for each step of the procedure.

CHAPTER 3: RESULTS

3.1.In-Silico Studies

3.1.1. ELM (Eukaryotic Linear Motif) & ExPASy (Expert Protein Analysis System)

The VSTM5 protein encompasses five distinct domains; among them being the immunoglobulin, (Ig) and signaling lymphocytic activation molecule (SLAM) (CD150) domains (Figure 8). Upon conducting a protein scan of the VSTM5 cytoplasmic domain, we observed that Tyrosine kinases were anticipated to bind with this area (Figure 7).

3.1.2. Protein – Protein Docking (HADDOCK)

The molecular docking technique is a valuable computational approach that predicts potential interactions between biomolecules and chemical compounds. Within this technique, protein-protein docking focuses on exploring interactions between protein interfaces, offering preliminary yet reliable insights. One widely used protein-protein docking method is HADDOCK (High Ambiguity Driven protein-protein Docking), which provides HADDOCK Score and Z-score as evaluation metrics. Negative scores indicate a higher likelihood of protein binding affinity and data reliability, respectively. In our study, we used the PVR2 binding of the VSTM3-TIGIT protein, which has been previously reported as a control. We conducted docking simulations using HADDOCK to explore the interactions between various natural cytotoxicity immune receptors (such as 2DL2, FC-Gamma, 2DL4, KIR2DS2, NKG2A, PVR (CD155), Nkp30, and NKp46) and members of the VSTM protein family. The results, summarized in Table 7, revealed that VSTM3 and VSTM5 proteins exhibited similar binding affinities with the investigated natural cytotoxicity receptors, unlike VSTM1, VSTM2, and VSTM4. These findings suggest a potential shared natural cytotoxicity receptor binding affinity between VSTM5 and VSTM3, supported by their high structural similarity and binding profiles. While further confirmation through *in vitro* and *in vivo* studies is required, our results indicate that VSTM5 could be a promising candidate for immune checkpoint-associated cancer treatments.

Table 10. Protein – Protein Docking Results: HADDOCK and Z-scores of VSTM family protein binding prediction to selected natural cytotoxicity receptors. Negative HADDOCK and Z scores are highlighted in bold.

VSTM Family	Protein Name	HADDOCK Score	Z-Score
VSTM 1	NK2DL2	112.1 +/- 27.5	-1.7
	Fc-Gamma Receptor III	12.1 +/- 7.5	-2.2
	NK2DL4	117.2 +/- 19.2	-1.7
	KIR2DS2	110.8 +/- 14.9	-2.2
	NKG2A	70.0 +/- 20.8	-1.6
	NKp46	80.7 +/- 8.1	-1.8
VSTM 2	NK2DL2	107.0 +/- 22.1	-1.5
	Fc-Gamma Receptor III	92.6 +/- 10.4	-2.0
	NK2DL4	121.1 +/- 33.4	-1.9
	KIR2DS2	129.1 +/- 15.7	-2.3
	NKG2A	161.4 +/- 20.3	-1.4
	NKp46	121.5 +/- 11.8	-2.1
VSTM 3	**NK2DL2***	**-34.5 +/- 10.9**	**-1.1**
	Fc-Gamma Receptor III*	**-56.2 +/- 5.4**	**-1.7**
	NK2DL4*	**-41.1 +/- 9.9**	**-1.4**
	KIR2DS2*	**-38.6 +/- 12.1**	**-1.4**
	NKG2A*	**-65.0 +/- 4.3**	**-2.1**
	NKp46*	**-72.9 +/- 2.4**	**-2.0**
	PVR (CD155)*	**-26.2 +/- 10.8**	**-2.1**
VSTM 4	NK2DL2	151.9 +/- 16.6	-1.6
	Fc-Gamma Receptor III	106.3 +/- 3.6	-1.8
	NK2DL4	138.7 +/- 16.0	-1.9
	KIR2DS2	184.8 +/- 21.5	-1.8
	NKG2A	150.7 +/- 10.9	-1.8
	NKp46	141.8 +/- 7.7	-1.9
VSTM 5	**NK2DL2***	**- 28.2 +/- 6.0**	**- 2.1**
	Fc-Gamma Receptor III*	**- 35.3 +/- 11.9**	**- 1.7**
	NK2DL4*	**- 14.3 +/- 17.8**	**- 1.5**
	KIR2DS2	25.0 +/- 50.8	- 1.3
	NKG2A*	**- 73.7 +/- 11.3**	**- 2.5**
	NKp46*	**- 43.4 +/- 17.4**	**-1.3**

3.2.*In vitro Studies*

3.2.1. Cell Culture

The cell culture experiments conducted in this study have provided valuable insights into the behavior of cells under controlled laboratory conditions. HT29, LoVo, and HCT116 cell lines known to be CMS1 group cell lines were used as experimental groups, while CCD18-Co, a normal colon epithelial cell line, and A549, a lung cancer cell line known to have VSTM5 expression, were used as control cells (Figure 10).

These cells were opened, passaged, stocks were prepared for later use, and pellets were obtained from the cells for RNA isolation.

3.2.2. cDNA Synthesis

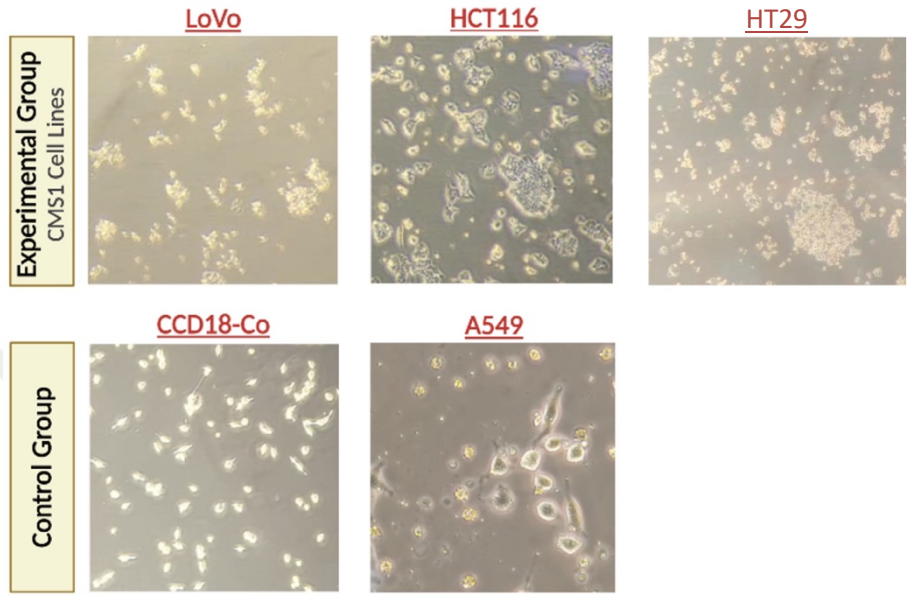

Figure 10**.** Cell Lines. The experimental group consisted of well-known cell lines HT29, LoVo, and HCT116, which are recognized as CMS1 subgroup cell lines. Meanwhile, the control group comprised CCD18-Co, a normal colon epithelial cell line, and A549, a lung cancer cell line known to express VSTM5.

Following the isolation of RNA from each cell line, the quality and quantity of the RNA samples were assessed using a Nanodrop spectrophotometer. The obtained measurements are presented in Table-4. In the present investigation, the A260/A280 ratio of the total RNA extracted from the cell lines exhibited values ranging from 1.90 to 2.2, suggesting high purity. Moreover, the A260/A230 ratio surpassed 1.80, indicating the absence of contaminants. The concentration of the total RNA varied from 468 ng/uL to 984 ng/uL, encompassing the range of values required for cDNA synthesis for template expression.

Due to the absence of identified contamination in the RNA samples, the cDNA synthesis process has proceeded using the same samples.

Table 11. RNA sample Nanodrop Measurements.

Cell Line	Concentration (ng/μL)	A260 / A230	A260 / A280
CCD18-Co	468 ng/μL	1,9	2,0
A529	984 ng/μL	2,18	1,8
LoVo	539 ng/μL	1,71	2,09
HCT116	1241 ng/μL	1,93	2,2
HT29	901 ng/μL	1,88	2,0

3.2.3. G418 Antibiotic Killing Curve with MTT

In order to ascertain the lethal dose (LD) at which G418 antibiotic induces complete cell death in the LoVo cell line, a range of concentrations, including 0 μg/mL, 10 μg/mL, 25 μg/mL, 50 μg/mL, 100 μg/mL, 200 μg/mL, 400 μg/mL, 600 μg/mL, 800 μg/mL, 1000 μg/mL, 1500 μg/mL, and 2000 μg/mL of G418, were administered to LoVo cells for a duration of 3 days. Subsequently, the cell survival rate was assessed. The results was subjected to comprehensive analysis, culminating in the determination of the LD50 value for G418, which was calculated to be 372.5 ug/mL and LD90 value as 3210 ug/mL (Figure 11).

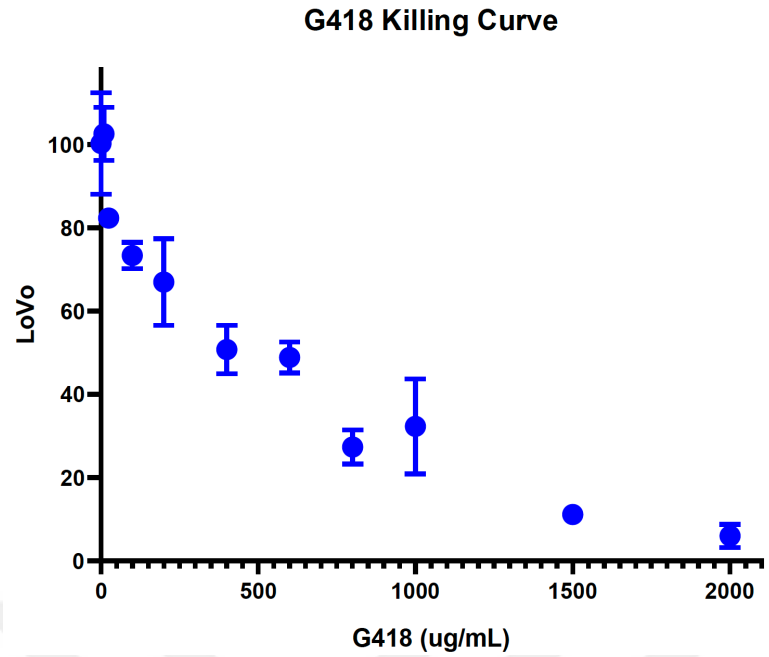

Figure 11. MTT survival graph. The MTT survival graph illustrates the cell viability responses of LoVo cells to varying concentrations of G418 antibiotic. The graph showcases the dose-dependent cytotoxic effects of G418, with cell survival rates expressed as a percentage relative to untreated control cells. Error bars represent standard deviations from multiple experimental replicates.

3.2.4. PCR & qPCR and Agarose Gel Electrophoresis

3.2.4.1. qPCR

The basal expression levels of VSTM5 in the human cancer cell lines were assessed using quantitative polymerase chain reaction (qPCR). Prior to conducting qPCR experiments, we aimed to select the most suitable housekeeping gene for our experiments.

Therefore, we performed RT-qPCR experiments at different time points using 18S rRNA and β-actin housekeeping genes. We opted to conduct our analyses using the 18S rRNA housekeeping gene due to its lower variation among the cell lines.

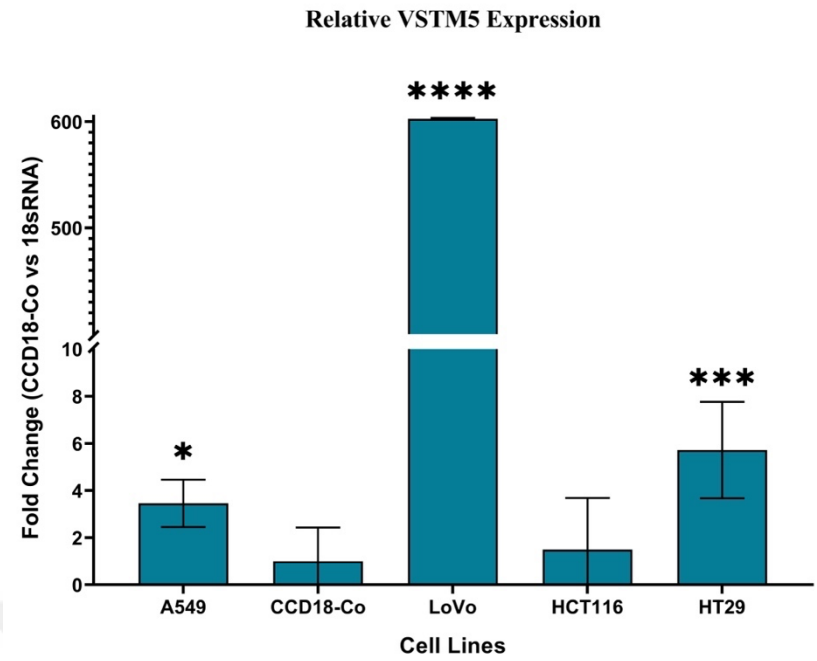

Figure 12. The qPCR results depict the expression of VSTM5 in colon cancer cell lines. The fold change values are graphed in the bar chart, enabling the comparison of endogenous VSTM5 expression levels among different cell lines. The significance of these differences is indicated by the accompanying p-values ($p < 0.05$, ** $p < 0.01$, *** $p < 0.001$, **** $p < 0.0001$). The study involved n=6 for the HT29 cell line and n=12 for all other cell lines. Furthermore, the t-test results were employed to assess the variance in A8 expression concerning CCD18-Co. This figure provides a visual representation of the quantitative PCR outcomes, which are crucial in understanding the relative VSTM5 expression levels in different cell lines.

The cycle threshold (Ct) values of all samples were analyzed to determine the fold change (2^-ΔΔCt) relative to the expression of the 18S Ribosomal RNA , which served as the housekeeping gene (Figure 12).

3.2.4.2. High Fidelity PCR

High-fidelity polymerase chain reaction (PCR) is a technique that utilizes a DNA polymerase enzyme with a low error rate to faithfully duplicate a specific DNA sequence with exceptional accuracy.

The PCR products derived from the amplification of the VSTM5 gene were examined using agarose gel electrophoresis. A 1% agarose gel stained with ethidium

bromide (EtBr) was utilized for visualization. Within the gel, a distinct band representing the VSTM5 product with a size of 2909 base pairs (bp) were clearly observed (Figure 13).

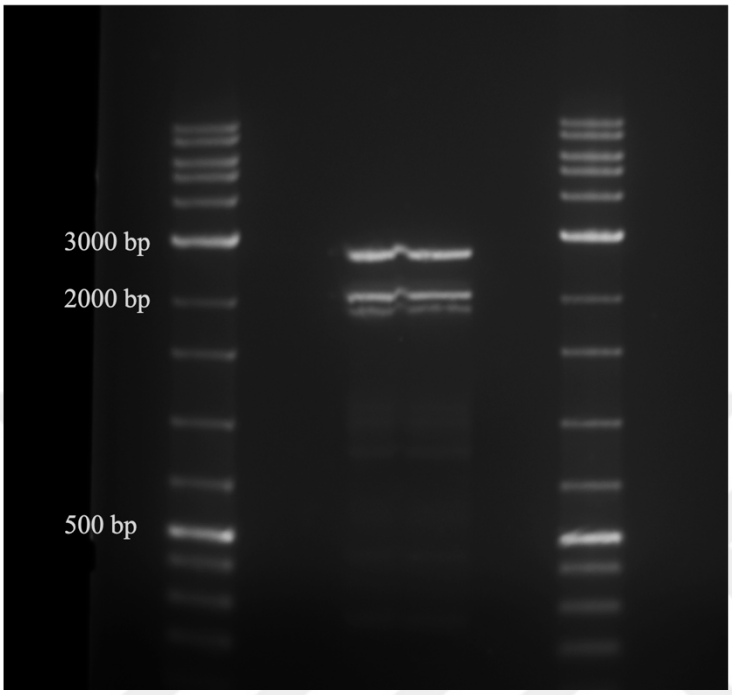

Figure 13. Hi-Fidelity PCR Result: The PCR products derived from the amplification of the VSTM5 gene were examined using agarose gel electrophoresis. A 1% agarose gel stained with ethidium bromide (EtBr) was utilized for visualization. Within the gel, a distinct band representing the VSTM5 product with a size of 2909 base pairs (bp) were clearly observed.

3.2.4.3. Touchdown (TD) PCR

Touchdown Polymerase Chain Reaction (TD-PCR) is a prompt and efficacious technique that optimizes PCR outcomes by improving specificity, sensitivity, and yield without necessitating extensive adjustments or primer redesign.

This process commences by setting an initial annealing temperature higher than the anticipated melting temperature (Tm) of the primers and gradually lowering it in subsequent cycles. The difference in Tm between appropriate and inappropriate annealing results in an exponential twofold increase per cycle. TD-PCR is a commonly used technique in various PCR protocols, including those for screening single nucleotide polymorphisms, constructing cDNA libraries, and conducting reverse transcriptase-dependent PCR. Its utility is particularly noteworthy for amplifying

challenging templates and can also augment specificity and product formation in standard applications. During the execution of the Touchdown PCR (TD-PCR) protocol, the PCR products were analyzed by running them on a 2% agarose gel (Figure 14). The gel electrophoresis revealed the presence of the expected bands in the gel. The reaction control band, represented by the 18S ribosomal RNA, appeared at the correct molecular weight (WM), confirming the functionality of the PCR reaction. Additionally, the specific band corresponding to the VSTM5 coding sequence (CDS) was also observed, indicating the successful amplification of the target gene.

3.2.4.4. Agarose Gel Electrophoresis

Subsequently, we investigated the RNA expression levels of VSTM5 in our panel of human cancer cell lines. Interestingly, CCD18-Co cell lines, representative of normal colonic epithelial cells, exhibited elevated levels of VSTM5 expression compared to colon cancer cell lines (Figure 15).

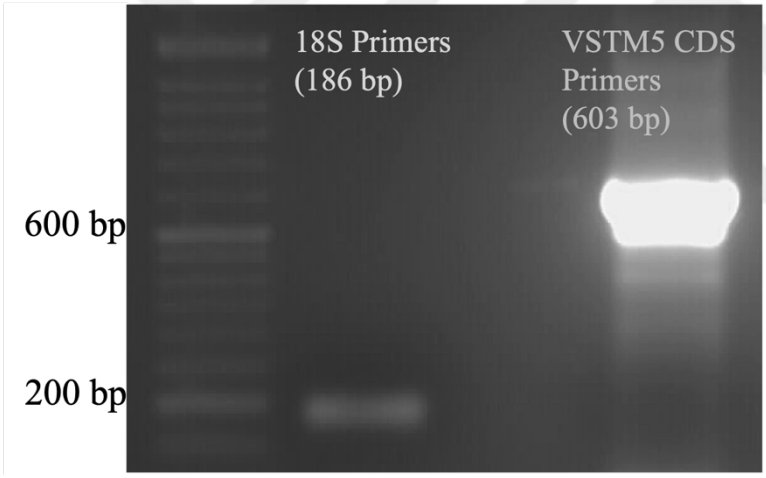

Figure 14. Touchdown PCR Result: The examination of the Touchdown PCR products, resulting from the amplification of the VSTM5 gene, was conducted through the implementation of agarose gel electrophoresis. The visualization process entailed the utilization of a 2% agarose gel, which was subjected to the staining properties of ethidium bromide (EtBr). Notably, the resulting gel exhibited a conspicuous band, indicative of the VSTM5 product, with a size measuring 603 base pairs (bp).

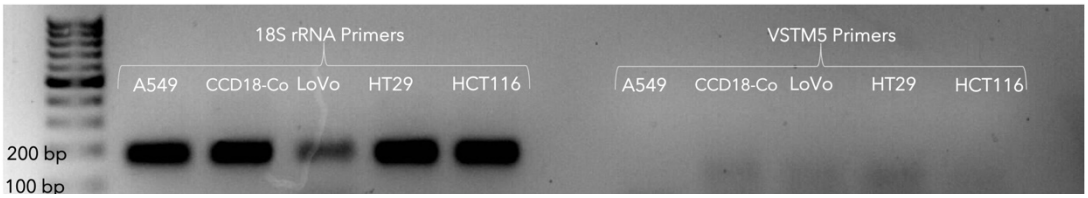

Figure 15. Agarose gel electrophoresis results. The amplified PCR products of the VSTM5 gene were visualized on a 1.5% agarose gel stained with ethidium bromide (EtBr). The gel included a VSTM5 product (146 bp) band and in the control group, a band corresponding to the 18S rRNA (186 bp) was observed.

3.2.5. Molecular Cloning

3.2.5.1. Heat Shock Transformation and Plasmid Isolation

Following the transformation procedure, the DH5α cells were grown on LB Agar supplemented with ampicillin for selection (Figure 17).

The most robust colonies developed after the incubation period was carefully selected, and subsequent plasmid isolation was carried out.

The pcDNA3-EGFP plasmid (Figure 16) was obtained following the 16-hour incubation of the selected colony in the LB medium, as depicted in Figure 16.

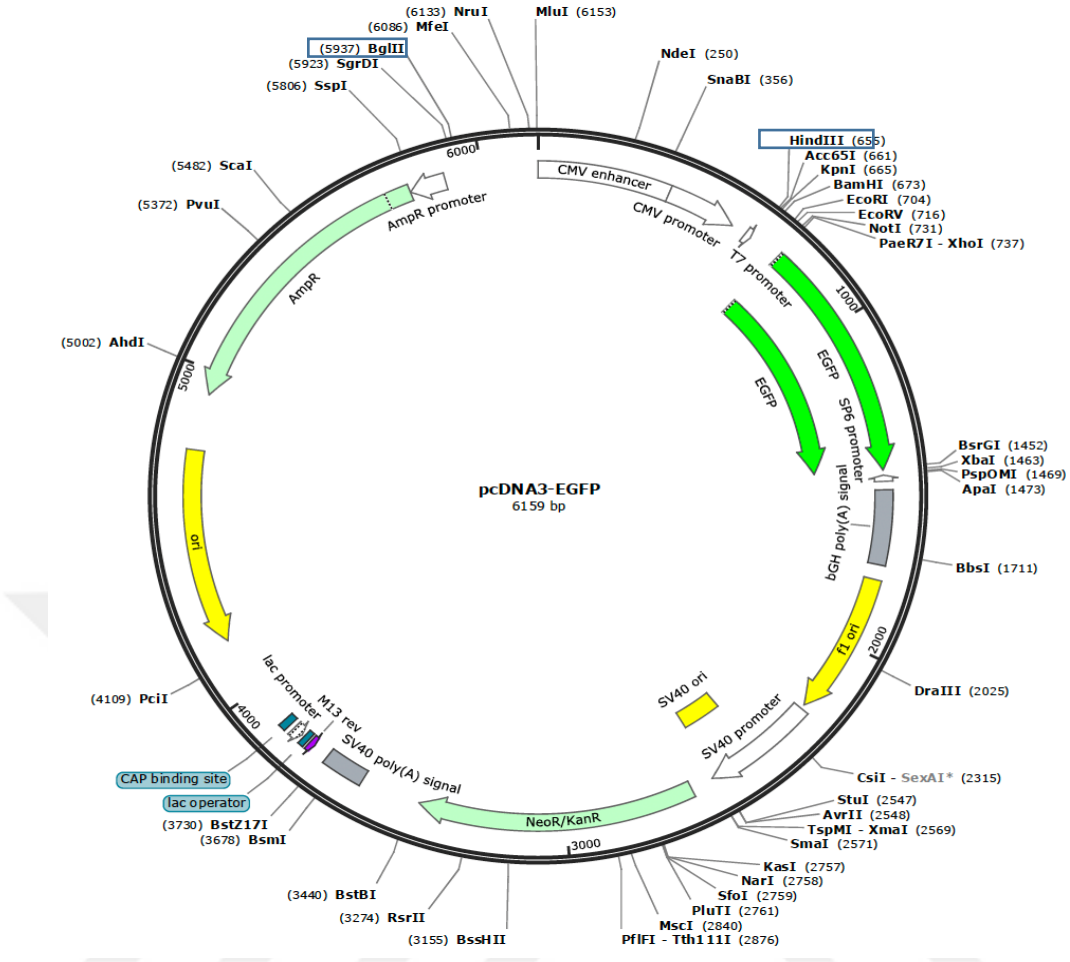

Figure 16. Structure of pcDNA3-EGFP plasmid. To investigate the effect of VSTM5 gene expression on the cell growth rate, we planned to clone the VSTM5 gene into the HCT116 cell line. To achieve this, we prepared the pcDNA3-EGFP.VSTM5 construct using BglII and HindIII double digestion.

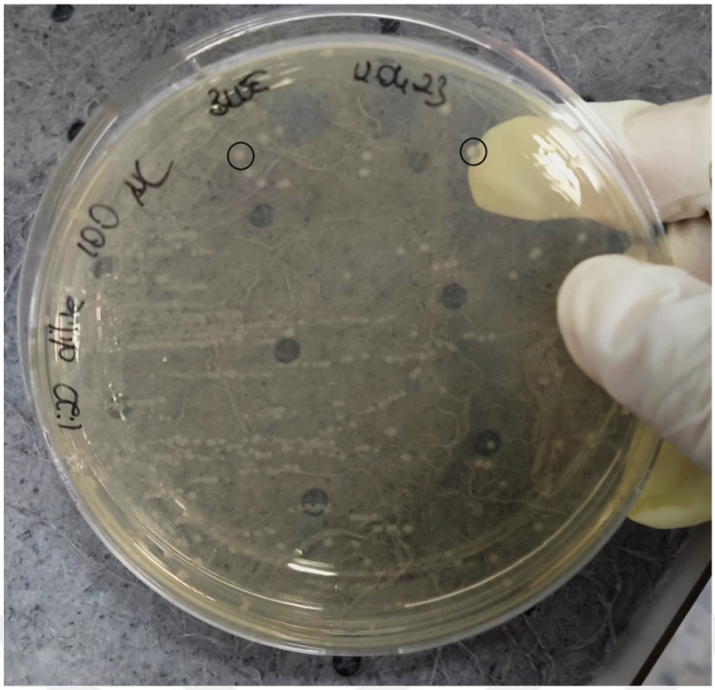

Figure 17. Transformed E.coli DH5α colonies. Following the transformation step, the bacteria were plated onto LB-agar supplemented with 100 µg/mL ampicillin and incubated overnight to facilitate the selection of bacteria carrying the plasmid. The presence of the ampicillin resistance gene in the plasmid genome enabled the formation of colonies by DH5a bacteria during the incubation period.

Subsequently, the purity and concentration of the isolated plasmid were assessed using Nanodrop spectrophotometry, as illustrated in Table 9.

Table 12. Nanodrop measurement of isolated plasmids.

Colony Number	Concentration (ng/µL)	A260 / A230	A260 / A280
#1	789.93	2.12	1.94
#2	730.12	1.85	1.43
#3	692.86	2.12	1.96

3.2.5.2. Restriction Enzyme Digestion

pcDNA3-EGFP was subjected to digestion with the restriction enzymes *HindIII* and *BgIII* for cloning purposes. The digested plasmid was subsequently verified through agarose gel electrophoresis, as displayed in Figure 18.

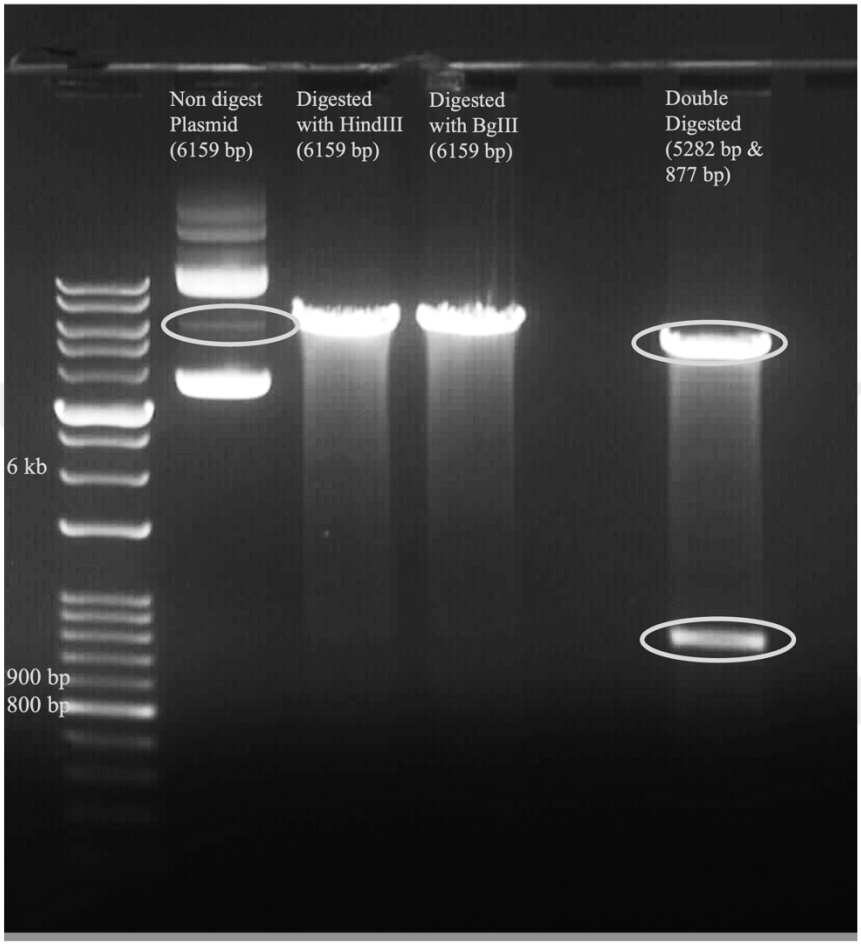

Figure 18. Agarose gel result of plasmid isolation. Circular, linear, and digested plasmids were loaded onto a 1% agarose gel at 1 ug and run at 120V.

3.2.5.3. Transformation and Colony Selection

Following the introduction of the VSTM5^{+}pcDNA3-EGFP plasmid into the *E. coli* DH5α strain to facilitate efficient propagation, the bacterial culture was subsequently spread onto LB agar supplemented with 100 µg/mL ampicillin. An overnight incubation was conducted to foster the enrichment of bacterial populations harboring the introduced plasmid. The presence of the ampicillin resistance gene within the plasmid conferred antibiotic resistance to the DH5α bacterial strain, thereby allowing for colony formation during the incubation period. One of the selected colonies is shown in Figure 19.

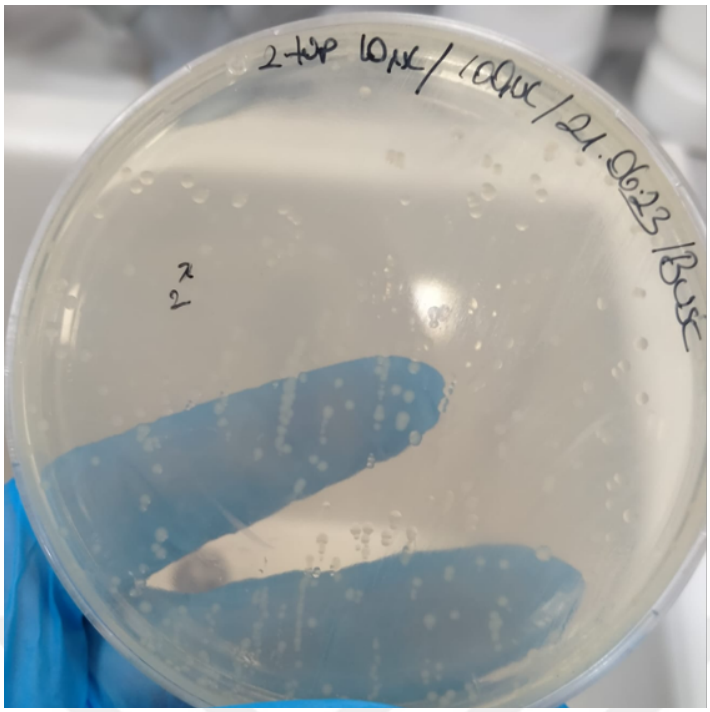

Figure 19. Bacterial Colony Selection Following Transformation and Incubation. An agar plate utilized in the experiment after bacterial transformation and 24-hour incubation. A single colony was selected (labelled) from this plate for further analysis.

The colony marked in Figure 19 was isolated after 16 hours of incubation in LB medium.

3.2.5.4. Colony Isolation

After performing the isolation of plasmids on LB agar plates, their concentrations were determined using a Nanodrop spectrophotometer, and the results are presented in Table 13. To investigate whether these isolated plasmids from eight different colonies contained the VSTM5 gene, we conducted PCR reactions utilizing CDS primers and subsequently analyzed the generated products on a 2% agarose gel. The CDS primers were specifically designed to yield a product with a size of 603 base pairs if VSTM5 is present.

Table 13. Concentration of isolated VSTM5$^{(+)}$pcDNA3-EGFP.

Colony Number	Concentration (ng/μL)	A260 / A230	A260 / A280
#1	341.466	2.08	2.18
#2	344.296	2.07	2.18
#3	358.161	2.07	2.17
#4	361.367	2.04	2.06
#5	365.034	2.13	1.94
#6	387.909	2.06	1.93
#7	402.078	2.01	2.07
#8	406.136	2.02	1.94

3.2.5.5. PCR amplification of cloned VSTM5

To verify VSTM5 cloning results, we amplified isolated clones with VSTM5 primers, followed by running of PCR products in an agarose gel (Figure 20). Figure shows PCR products with anticipated molecular weight for VSTM5 (603bp) for each of the isolated plasmid from clones listed in Table 13.

Figure 20. PCR Confirmation of Gene Insertion. An agarose gel image confirming the results of PCR amplification of gene VSTM5 in pcDNA3. 603 bp product in PCR reactions from eight separate colonies. This outcome indicates the successful insertion of the VSTM5 into the pcDNA3 plasmid.

The presence of these bands confirmed that the isolated plasmids contained the VSTM5 gene. Following this verification, we stored these VSTM5-positive plasmids at -20°C, preserving them for use in our subsequent transfection protocol.

3.2.5.6. Transfection of mammalian expression vector into CMS1 colon cancer cell line LoVo

Due to the absence of optimized electroporation protocols for LoVo cell lines in the literature, a series of electroporation experiments were conducted using different pulse durations and voltage settings. As a result of these experiments, protocols yielding viable cells and fluorescent microscopy images of post-electroporation cells are presented in Figure 21. The obtained live cells were subsequently placed in selective growth media, with the expectation that non-transfected cells would perish, while successfully transfected cells would survive due to the presence of an antibiotic resistance gene in the plasmid. This study provides valuable insights into the development of electroporation protocols for LoVo cell lines and the examination of live cell outcomes.

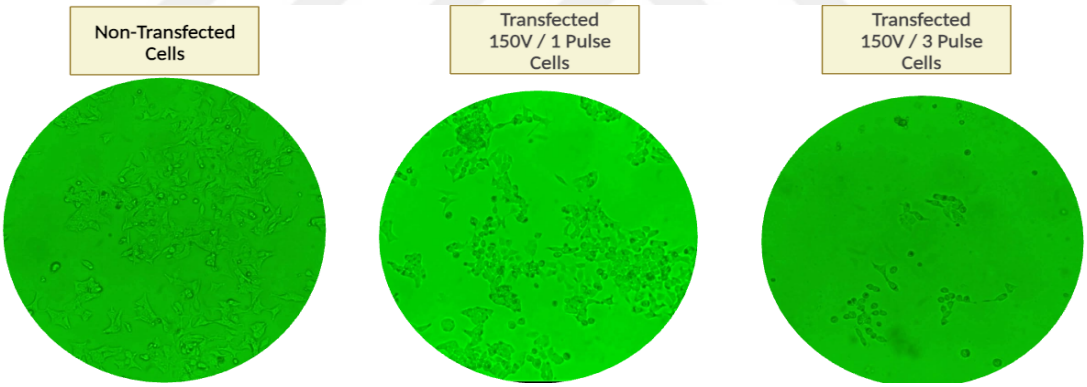

Figure 21. Fluorescence Microscopy Images. Fluorescence microscopy images were captured at 40X magnification, showcasing non-transfected cells, 150 Volt 1 pulse transfected cells, and 150 Volt 3 pulse transfected cells.

CHAPTER 4: DISCUSSION

Colon cancer is considered high incidence among cancers due to its high global incidence rates compared to other types of cancer (Dasari et al., 2022). As an alternative to standard classification, molecular classification of colon cancer patients has been suggested to offer advantages in predicting prognosis and guiding treatment approaches. The CMS1 group of colon cancer includes patients with a strong immune response, characterized by high immune cell infiltration into the tumor tissue (Guinney et al., 2015). Using *in silico* methods, we identified an 11 gene signature that is associated with the survival of colon cancer patients. Among these genes, 5 of them are under further investigation with subsequent projects, out of which 4 of them associates with CMS1 group of patients. One of these genes is VSTM5 and our results previously demonstrated that patients with high VSTM5 expression is associated with longer disease specific survival than patients with low VSTM5 expression. To elucidate the mechanism for this observation, we initially investigated the VSTM gene family. Previous studies established that several members of the VSTM gene family are associated with cancer and associate with anti-tumor immune functions. One member of this gene family, VSTM3 (TIGIT), has been identified as an immune checkpoint with ongoing therapeutic drug trials. Despite the abundance of research on the VSTM gene family, studies focusing specifically on VSTM5 are scarce. Proposed functions of VSTM5 in the literature include its involvement in neuronal morphology and its effect on filopodia formation. In a recent study, VSTM5 expression was found to inhibit T cell proliferation and B cell responses in mice, suggesting its potential as an immune checkpoint inhibitor (Oludada et al., 2022).

In our analysis aimed at predicting the function of VSTM5, we observed that VSTM5 has tyrosine kinase binding sites in its cytoplasmic region, which is shared among many signaling molecules with immunoregulatory functions

. The immune system is a complex network comprised of cells and molecules that function to protect the body against foreign substances and pathogens. The immune system's balance is maintained by immune checkpoints, which prevent excessive immune responses and tissue damage.

Discovering new immune checkpoints is crucial in the development of effective immunotherapy methods for treating cancer, autoimmune diseases, and infectious diseases. The exploration of this enigmatic genetic entity and its potential function as

an immune checkpoint represents an innovative avenue for prospective research. The revelations of this investigation may furnish valuable insights into the formulation of pioneering immunotherapeutic modalities aimed at modulating immune responses. It is imperative to acknowledge that the scope of the study is restricted by the ambiguity surrounding the function of the gene under scrutiny. Consequently, to ascertain the exact function of the gene and its probable role as an immune checkpoint, further investigations are required. Accordingly, it is crucial to carry out more research to examine the gene's expression patterns and protein-protein interactions in diverse immune cells and tissues.

Our findings suggest that only one of these proteins, namely STAT3, binds with Tyrosine (Y) 175, a component located within the cytoplasmic domain of VSTM5. It has long been established that activation of NK cell cytotoxic function is facilitated by tyrosine phosphorylation, thereby indicating the significance of this binding. At the same time, the STAT3 molecule, which is known to be activated by serine/tyrosine phosphorylation (Rébé et al., 2013), is also involved in NK activation (Phatarpekar et al., 2010), revealing the importance of tyrosine phosphorylation for both VSTM5 and STAT3. Another protein that we have determined to bind to the cytoplasmic region of VSTM5 is the casein kinase-2 (CK2*)* protein. Inhibition of the CK2 protein is known to significantly increase NK cell-mediated cancer cell killing (Kim et al., 2008).

However, for VSTM5 to positively affect survival, it must either enhance the immune system response or slow the rate at which cancer cells divide. Initially, we aimed to investigate the effect of VSTM5 on cell growth rate and planned to explore its effect on the immune system in future studies. Considering the existing literature, we identified the CMS1 group of colon cancer cell lines and obtained LoVo, HCT116, and HT29 cell lines. Since no cell line in the literature has been studied for VSTM5 expression, we used the A549 lung cancer cell line, which showed the highest VSTM5 expression in Expression Atlas, as a positive control. To assess the difference in VSTM5 expression between healthy colon cells and CMS1 group colon cancer cells, we used the CCD18-Co cell line to represent healthy colon epithelium. Through qPCR experiments involving these cell lines, we found that VSTM5 expression was higher in healthy colon epithelium than in CMS1 group colon cancer cell lines and lung cancer cell lines. The lower expression observed in CMS1 group colon cancer cells compared to healthy colon epithelial cell lines was expected. The observed lower expression of VSTM5 in CMS1 group colon cancer cells compared to healthy colon

epithelium is consistent with the higher survival rates observed in patients with high VSTM5 expression. This suggests that VSTM5 may play a crucial role in regulating cell growth and immune responses in colon cancer. Further investigations are needed to fully understand the underlying mechanisms and biological significance of VSTM5 expression in colon cancer and its impact on patient outcomes.

Our results were inconsistent for the LoVo cell line Ct values and fold changes , which led to its exclusion from the qPCR analysis. We speculate that the inconsistency is due to the unhealthy condition of the cells, which might suggest a possible mycoplasma contamination.

Furthermore, we discussed the advantages of using high-fidelity polymerases over Taq polymerase in PCR experiments for cloning protocol, highlighting their superior accuracy in minimizing errors during DNA replication. In contrast to Taq polymerase, high-fidelity polymerases employ two mechanisms to minimize errors during DNA replication. Firstly, their binding sites have a stronger affinity for the correct nucleotide compared to Taq polymerase. Additionally, high-fidelity polymerases possess an additional domain that acts as a proofreading mechanism, capable of detecting structural abnormalities caused by mismatches and performing 3'-5' exonuclease activity to correct errors during DNA synthesis. When it comes to generating amplicons for highly sensitive applications like cloning and sequencing, high-fidelity DNA polymerases offer a reliable and precise alternative to the conventional Taq polymerase-based PCR method.

Our future experiments involve investigating the effect of altered VSTM5 expression on cell growth rate by transiently transfecting the VSTM5 gene into the HCT116 cell line, which exhibited the lowest VSTM5 expression among the experimental group of cell lines. For this purpose, the pcDNA3-EGFP plasmid required for VSTM5 gene transfection was successfully amplified and isolated. As our study's planned experiments are ongoing, our findings regarding the effect of VSTM5 gene expression on the growth of CMS1 group colon cancer cell lines are currently incomplete. Although we have successfully cloned the CDS of VSTM5 gene into a mammalian expression vector, we have yet introduced this construct into CMS1 colon cancer cells by electroporation for transient cloning. For future directions, we plan to select cells containing cloned VSTM5 and a compare the growth rates of parental cells with VSTM5-positive cells using MTT or CFSE based flow cytometric viability assays.

CHAPTER 5: CONCLUSION

Our research team conducted *in silico* studies to investigate the potential correlation between the expression of the VSTM5 gene and long-term survival in CMS1 group colon cancer patients. The results showed a positive correlation between the high expression of the VSTM5 gene and better long-term survival in CMS1 group colon cancer patients, suggesting a possible role for the gene in regulating cell division or influencing the immune system. While the exact function of the VSTM5 gene in cancer is unknown, the current literature suggests that it may act as an immune checkpoint.

We also analyzed the expression of the VSTM5 gene in CMS1 group colon cancer cell lines and healthy colon epithelial cell line. The analysis revealed that higher expression levels of the VSTM5 gene in healthy colon epithelium than in CMS1 group colon cancer cell lines, indicating a potential role for the gene in maintaining healthy colon epithelial cells. However, differences in VSTM5 expression were also observed within the CMS1 group of colon cancer cell lines. The LoVo cell line was excluded from the study due to inconsistent qPCR results, suggesting that the cells used may not be healthy.

It is important to note that the experiments outlined in the thesis are ongoing. Future work will focus on comparing cell growth rates following cloning studies, which will provide additional insights into the role of the VSTM5 gene in cell proliferation.

This study highlights the investigation of the VSTM5 gene and its impact on colon cancer survival. The findings suggest that the gene may regulate cell division or influence the immune system. It provides a foundation for further research aimed at elucidating the underlying mechanisms and functional significance of the VSTM5 gene in cancer. Further research is needed to fully understand the underlying mechanisms and functional significance of the VSTM5 gene in cancer. Ongoing experiments and future studies will provide additional insights into the role of the VSTM5 gene in cell proliferation and contribute to the development of personalized treatment strategies for colon cancer patients.

REFERENCES

Al Dow, M., Silveira, M.A.D., Poliquin, A., Tribouillard, L., Fournier, É., Trébaol, E., Secco, B., Villot, R., Tremblay, F., Bilodeau, S., Laplante, M., 2021. *Control of adipogenic commitment by a STAT3-VSTM2A axis*. American Journal of Physiology-Endocrinology and Metabolism Vol. 320, pp. E259–E269.

Berg, K.C.G., Eide, P.W., Eilertsen, I.A., Johannessen, B., Bruun, J., Danielsen, S.A., Bjørnslett, M., Meza-Zepeda, L.A., Eknæs, M., Lind, G.E., Myklebost, O., Skotheim, R.I., Sveen, A., Lothe, R.A., 2017. *Multi-omics of 34 colorectal cancer cell lines - a resource for biomedical studies.* Mol Cancer Vol. 16, pp. 116.

Chauvin, J.M., Zarour, H.M., 2020. *TIGIT in cancer immunotherapy*. J Immunother Cancer Vol. 8, pp. 957.

Clinical Studies on TIGIT [Online], Avaible at: https://clinicaltrials.gov/ct2/results/browse?term=TIGIT&recrs=abdef&brwse=cond_alpha_all. [Accessed: 10.08.2023],

Dasari, A., Johnson, B., Parseghian, C., Raghav, K.P., Kopetz, S., 2022. Colorectal Cancer, in: Kantarjian, H.M., Wolff, R.A., Rieber, A.G. (Eds.), The MD Anderson Manual of Medical Oncology, 4e. McGraw Hill Education, New York, NY.

Dong, Y., Zhang, Y., Kang, W., Wang, G., Chen, H., Higashimori, A., Nakatsu, G., Go, M., Tong, J.H., Zheng, S., To, K.F., Sung, J.J., Yang, X., Ng, S.S., Yu, J., 2019. *VSTM2A suppresses colorectal cancer and antagonizes Wnt signaling receptor LRP6*. Theranostics Vol. 9, pp. 6517–6531.

Fichtner, M., Bozkurt, E., Salvucci, M., McCann, C., McAllister, K.A., Halang, L., Düssmann, H., Kinsella, S., Crawford, N., Sessler, T., Longley, D.B., Prehn, J.H.M., 2020. *Molecular subtype-specific responses of colon cancer cells to the SMAC mimetic Birinapant.* Cell Death Dis Vol.11, pp.1020.

González-Sarrías, A., Espín-Aguilar, J.C., Romero-Reyes, S., Puigcerver, J., Alajarín, M., Berná, J., Selma, M.V., Espín, J.C., 2022. *Main Determinants Affecting the Antiproliferative Activity of Stilbenes and Their Gut Microbiota Metabolites in Colon Cancer Cells: A Structure–Activity Relationship Study*. Int J Mol Sci Vol. 23, pp. 15102.

Guinney, J., Dienstmann, R., Wang, X., De Reyniès, A., Schlicker, A., Soneson, C., Marisa, L., Roepman, P., Nyamundanda, G., Angelino, P., Bot, B.M., Morris,

J.S., Simon, I.M., Gerster, S., Fessler, E., De Sousa .E Melo, F., Missiaglia, E., Ramay, H., Barras, D., Homicsko, K., Maru, D., Manyam, G.C., Broom, B., Boige, V., Perez-Villamil, B., Laderas, T., Salazar, R., Gray, J.W., Hanahan, D., Tabernero, J., Bernards, R., Friend, S.H., Laurent-Puig, P., Medema, J.P., Sadanandam, A., Wessels, L., Delorenzi, M., Kopetz, S., Vermeulen, L., Tejpar, S., 2015. *The consensus molecular subtypes of colorectal cancer*. Nat Med Vol. 21, pp. 1350–1356.

Guo, X., Zhang, Y., Wang, P., Li, T., Fu, W., Mo, X., Shi, T., Zhang, Z., Chen, Y., Ma, D., Han, W., 2012. *VSTM1-v2, a novel soluble glycoprotein, promotes the differentiation and activation of Th17 cells.* Cell Immunol Vol. 278, pp. 136–142.

Türkiye Halk Sağlığı Kurumu, 2017, Hacıkamiloğlu, E., Gültekin, M., Boztaş, G., Dündar, S., Utku, E.Ş., Kavak Ergün, A., Sevinç, A., Tütüncü, S., Seymen, E., Türkiye Kanser İstatistikleri, [Online], Avaible at: www.kanser.gov.tr/daire-faaliyetleri/kanser-istati. [Accessed: 12.07.2022],

Han, Y., Chen, W., Song, Y., Yuan, Y., Li, Z., Zhou, Y., Liu, T., Han, D., Mi, X., Li, M., Wang, G., Zhong, L., Zhou, J., Guo, X., 2020. *Proteomic Analysis of Preoperative CSF Reveals Risk Biomarkers of Postoperative Delirium*. Front Psychiatry Vol. 11.

Harjunpää, H., Guillerey, C., 2020. *TIGIT as an emerging immune checkpoint*. Clin Exp Immunol Vol. 200, pp.108–119.

Ishak, S.F., Rajab, N.F., Basri, D.F., 2023. *Antiproliferative Activities of Acetone Extract From Canarium Odontophyllum (Dabai) Stem Bark Against Human Colorectal Cancer Cells.* Dose-Response Vol. 21.

Johnston, R.J., Comps-Agrar, L., Hackney, J., Yu, X., Huseni, M., Yang, Y., Park, S., Javinal, V., Chiu, H., Irving, B., Eaton, D.L., Grogan, J.L., 2014. *The immunoreceptor TIGIT regulates antitumor and antiviral CD8(+) T cell effector function.* Cancer Cell Vol. 26, pp. 923–937.

Keller, D.S., Windsor, A., Cohen, R., Chand, M., 2019. *Colorectal cancer in inflammatory bowel disease: review of the evidence.* Tech Coloproctol Vol. 23, pp. 3–13.

Keum, N., Giovannucci, E., 2019. *Global burden of colorectal cancer: emerging trends, risk factors and prevention strategies*. Nat Rev Gastroenterol Hepatol Vol. 16, pp. 713–732.

Kim, H.R., Kim, K., Lee, K.H., Kim, S.J., Kim, J., 2008. *Inhibition of casein kinase 2 enhances the death ligand- and natural kiler cell-induced hepatocellular carcinoma cell death*. Clin Exp Immunol Vol.152, pp. 336.

Knudson, A.G., 1985. *Hereditary Cancer, Oncogenes, and Antioncogenes.* Cancer Res. Vol. 45(4), pp. 1437-43.

Kuipers, E.J., Grady, W.M., Lieberman, D., Seufferlein, T., Sung, J.J., Boelens, P.G., Van De Velde, C.J.H., Watanabe, T., 2015. *Colorectal cancer.* Nat Rev Dis Primers Vol. 1, pp. 1–25.

Lee, A.R., Kim, S., Ko, K.W., Park, C.S., 2017. *Differential effects of N-linked glycosylation of Vstm5 at multiple sites on surface expression and filopodia formation.* PLoS One Vol. 12.

Lee, A.R., Ko, K.W., Lee, H., Yoon, Y.S., Song, M.R., Park, C.S., 2016. *Putative cell adhesion membrane protein Vstm5 regulates neuronal morphology and migration in the central nervous system.* Journal of Neuroscience Vol. 36, pp.10181–10197.

Li, T., Guo, X., Wang, W., Mo, X., Wang, P., Han, W., 2015. *Vset and transmembrane domain containing 1 is silenced in human hematopoietic malignancy cell lines with promoter methylation and has inhibitory effects on cell growth*. Mol Med Rep Vol. 11, pp. 1344–1351.

Li, T., Wang, W., Chen, Y., Han, W., 2013. *Preparation and Characterization of Monoclonal Antibodies Against VSTM1.* Monoclon Antib Immunodiagn Immunother Vol. 32, pp. 283.

Liu, H., Zhang, Z., Zhen, P., Zhou, M., 2021. *High Expression of VSTM2L Induced Resistance to Chemoradiotherapy in Rectal Cancer through Downstream IL-4 Signaling.* J Immunol Res Vol. 2021, pp. 1–17.

Mukai, M., Uchida, K., Okubo, T., Takano, S., Matsumoto, T., Satoh, M., Inoue, G., Takaso, M., 2021. *Regulation of Tumor Necrosis Factor-α by Peptide Lv in Bone Marrow Macrophages and Synovium.* Front Med (Lausanne) Vol. 8, pp. 702126.

Ogino, S., Goel, A., 2008. *Molecular Classification and Correlates in Colorectal Cancer.* The Journal of Molecular Diagnostics Vol. 10, pp. 13–27.

Oludada, O.E., Idowu, T.O., Jeon, Y., Choi, I., 2022. *VSTM5 is a novel immune checkpoint that promotes oral tolerance of cell-mediated and antibody responses.* Biochem Biophys Res Commun Vol. 635, pp. 283–290.

Phatarpekar, P., Zhu, S., Denman, C.J., Nguyen-Jackson, N., Watowich, S.S., Cooper, L.J.N., Lee, D.A., 2010. *STAT3 Activation Promotes NK Cell Proliferation, NKG2D Expression, and NK Cell Antitumor Activity.* Blood Vol. 116, pp. 105

Pickhardt, P.J., Kim, D.H., Pooler, B.D., Hinshaw, J.L., Barlow, D., Jensen, D., Reichelderfer, M., Cash, B.D., 2013. *Assessment of volumetric growth rates of small colorectal polyps with CT colonography: a longitudinal study of natural history.* Lancet Oncol Vol. 14, pp. 711–720.

Rawla, P., Sunkara, T., Barsouk, A., 2019. *Epidemiology of colorectal cancer: incidence, mortality, survival, and risk factors.* Gastroenterology Review Vol. 14, pp. 89–103.

Rébé, C., Végran, F., Berger, H., Ghiringhelli, F., 2013. *STAT3 activation: A key factor in tumor immunoescape.* JAKSTAT Vol. 2, pp. e23010.

Ren, S., Gaykalova, D., Wang, J., Guo, T., Danilova, L., Favorov, A., Fertig, E., Bishop, J., Khan, Z., Flam, E., Wysocki, P.T., DeJong, P., Ando, M., Liu, C., Sakai, A., Fukusumi, T., Haft, S., Sadat, S., Califano, J.A., 2018. *Discovery and development of differentially methylated regions in human papillomavirus-related oropharyngeal squamous cell carcinoma.* Int J Cancer Vol. 143, pp. 2425–2436.

Search results < Expression Atlas < EMBL-EBI [WWW Document], n.d. URL https://www.ebi.ac.uk/gxa/search?geneQuery=%5B%7B%22value%22%3A%22A8MXK1%22%7D%5D&species=homo%20sapiens&conditionQuery=%5B%7B%22value%22%3A%22A549%22%7D%2C%7B%22value%22%3A%22HCT116%22%7D%2C%7B%22value%22%3A%22HT29%22%7D%2C%7B%22value%22%3A%22HT-29%22%7D%2C%7B%22value%22%3A%22LoVo%22%7D%2C%7B%22value%22%3A%22CCD18co%22%7D%2C%7B%22value%22%3A%22CCD18-co%22%7D%5D&bs=%7B%22homo%20sapiens%22%3A%5B%22CELL_LINE%22%5D%7D#baseline (accessed 10.30.22).

Secco, B., Camiré, É., Brière, M.A., Caron, A., Billong, A., Gélinas, Y., Lemay, A.M., Tharp, K.M., Lee, P.L., Gobeil, S., Guimond, J. V., Patey, N., Guertin, D.A., Stahl, A., Haddad, É., Marsolais, D., Bossé, Y., Birsoy, K., Laplante, M., 2017. *Amplification of Adipogenic Commitment by VSTM2A.* Cell Rep Vol. 18, pp. 93–106.

Shi, L., Ko, M.L., Abbott, L.C., Ko, G.Y.P., 2012. *Identification of Peptide lv, a novel putative neuropeptide that regulates the expression of L-type voltage-gated calcium channels in photoreceptors.* PLoS One Vol. 7.

Stanietsky, N., Rovis, T.L., Glasner, A., Seidel, E., Tsukerman, P., Yamin, R., Enk, J., Jonjic, S., Mandelboim, O., 2013. *Mouse TIGIT inhibits NK-cell cytotoxicity upon interaction with PVR.* Eur J Immunol Vol. 43, pp. 2138–2150.

Steevels, T.A.M., Lebbink, R.J., Westerlaken, G.H.A., Coffer, P.J., Meyaard, L., 2010. *Signal Inhibitory Receptor on Leukocytes-1 Is a Novel Functional Inhibitory Immune Receptor Expressed on Human Phagocytes*. The Journal of Immunology Vol. 184, pp.4741–4748.

Sung, H., Ferlay, J., Siegel, R.L., Laversanne, M., Soerjomataram, I., Jemal, A., Bray, F., 2021. Global Cancer Statistics 2020: *GLOBOCAN Estimates of Incidence and Mortality Worldwide for 36 Cancers in 185 Countries*. CA Cancer J Clin Vol. 71, pp. 209–249.

Testa, U., Pelosi, E., Castelli, G., 2018. Colorectal Cancer: *Genetic Abnormalities, Tumor Progression, Tumor Heterogeneity, Clonal Evolution and Tumor-Initiating Cells.* Medical Sciences Vol. 6, pp. 31.

Walther, A., Johnstone, E., Swanton, C., Midgley, R., Tomlinson, I., Kerr, D., 2009. *Genetic prognostic and predictive markers in colorectal cancer.* Nat Rev Cancer. Vol. 9, pp. 489–499

Wang, D., Li, Y., Liu, Y., He, Y., Shi, G., 2016. *Expression of VSTM1-v2 Is Increased in Peripheral Blood Mononuclear Cells from Patients with Rheumatoid Arthritis and Is Correlated with Disease Activity.* PLoS One Vol. 11, pp. e0146805

Wang, J., Manick, B., Renelt, M., Suin, J., Hansen, L., Person, A., Kalabokis, V., Wu, G., 2019. *VSTM4 is a novel negative regulator of T cell activation.* The Journal of Immunology Vol. 202.

Wang, X.F., En-Zhou, Li, D.J., Mao, C.Y., He, Q., Zhang, J.F., Fan, Y.Q., Wang, C.Q., 2021. *VSTM1 regulates monocyte/macrophage function via the NF-κB signaling pathway.* Open Medicine Vol. 16, pp. 1513.

Yu, X., Harden, K., Gonzalez, L.C., Francesco, M., Chiang, E., Irving, B., Tom, I., Ivelja, S., Refino, C.J., Clark, H., Eaton, D., Grogan, J.L., 2009. *The surface protein TIGIT suppresses T cell activation by promoting the generation of mature immunoregulatory dendritic cells.* Nat Immunol Vol. 10, pp. 48–57.

Zhang, S., Xiong, H., Yang, J., Yuan, X., 2022. *Pan-Cancer Analysis Reveals the Multidimensional Expression and Prognostic and Immunologic Roles of VSTM2L in Cancer.* Front Mol Biosci Vol. 8, pp. 792154

Zurit Levine, Galit Rotman, Liat Dassa, Ofer Levy, Gad S. Cojocaru, Amir Toporik, Yossef Kliger, Andrew Pow, S.L., 2016. (12) VSTM5 Antibodies, And Uses Thereof For Treatment Of Cancer, Nfectious Diseases And Immune Related Diseases, Patent Application Publication (10) Pub . No .: US 2016 / 0271610 A1 Patent Application Publication 1, 1–5.